CLUSTER ANALYSIS OF ACTIVE CAVERNS:
AKZO NOBEL — HENGELO BRINEFIELD

Topical Report RSI-1774
Revision 1

prepared for

Akzo Nobel Chemical
Boortorenweg 20
P.O. Box 25
Hengelo, GC 7550
Netherlands

April 2004

CLUSTER ANALYSIS OF ACTIVE CAVERNS:
AKZO NOBEL — HENGELO BRINEFIELD

Topical Report RSI-1774
Revision 1

by

5.1.2.e

RESPEC
P.O. Box 725
Rapid City, South Dakota 57709-0725
United States

prepared for

Akzo Nobel Chemical
Boortorenweg 20
P.O. Box 25
Hengelo, GC 7550
Netherlands

April 2004

TABLE OF CONTENTS

LIST OF TABLES

LIST OF FIGURES

1.0 INTRODUCTION

Recent compilation of information about cavern sizes and shapes, together with their locations, has revealed that some caverns in Akzo Nobel's Hengelo brinefield are closer to each other than anticipated. When just two caverns are in close proximity, the concern would be the relatively thin salt "wall" that separates the two caverns. Earlier numerical-modeling analyses by the BGR for Akzo Nobel demonstrates the stability for such side-by-side cavern arrangements where the oval-shaped caverns are either parallel or perpendicular to each other [BGR, 1998]. When three or more caverns are in proximity and the prescribed parallel or perpendicular arrangement of caverns is not applicable, the concern is not for the salt "wall," but rather, the salt "pillar" formed between the caverns. This report presents a methodology for assessing the stability of caverns in close proximity.

In dry salt mining, the primary stability concern is to leave enough salt underground in the form of pillars to continue to support the weight of the overburden. Before any mining, the weight of the overburden was uniformly borne by the undisturbed salt layer. After mining, the salt layer is interrupted at intervals of intersecting underground openings (think of intersecting tunnels). The salt between three or more intersecting openings forms a salt pillar. The mined openings themselves provide no support to the overburden; the rock-salt pillars must bear the weight of both the overburden directly above the pillar and the overburden directly above the surrounding openings. The weight borne by a pillar is proportional to the amount of salt removed (the extraction ratio); for greater amounts of extraction, greater amounts of weight must be borne by pillars.

This mining engineering method of calculating the weight borne by pillars is called the "tributary loading area" method. The total weight borne by a pillar divided by its cross-sectional area yields a descriptive rock-mechanics parameter called "stress;" in this case, the average vertical stress for the pillar. The magnitude of the average vertical stress is primarily a function of the extraction ratio (as determined in a plan or top view) and only secondarily a function of the height of the opening (as determined in a cross-sectional view). The vertical stress in the pillar can also be modified by any brine pressure acting on the mine (or solution-mining cavern) roof. The magnitude of the brine pressure depends on the height of the column of brine; at Hengelo, the brine column is always to the ground surface, so the brine pressure is nominally ½ the lithostatic rock stress. Thus engineering methods exist so pillars can be designed to ensure that the average vertical stresses do not exceed a predetermined magnitude, which is indicative of pillar stability.

The vertical stress, however, is not the only stress in pillars. Horizontal stresses also exist in the unmined rock, and some of the horizontal stress is transferred or develops in pillars after the pillars are isolated. The shape of a pillar (as defined by the ratios of its horizontal dimensions to height) strongly influences the magnitudes of internal horizontal stresses. At one extreme, a pillar that is thin and tall will develop virtually no internal horizontal stress; whereas, a short, thick (squat) pillar might develop relatively great internal horizontal stresses. In contrast to the vertical stress, where a large average vertical stress might suggest instability, greater horizontal stresses promote increased pillar stability. The internal horizontal stresses that develop away from the pillar edges provide confinement to the core of the pillar and make the entire salt pillar stronger (more resistant to weakening). The ratio between the vertical and horizontal stress magnitudes in a pillar is an indicator of the stability of the pillar.

The stresses in pillars, the cavern roof, and the surrounding rock can be determined by numerical modeling. Numerical modeling can be either two-dimensional or three-dimensional in space. Two-dimensional modeling of mining situations is typically either plane strain or axisymmetric. Relative to caverns, plane-strain modeling can be viewed as looking at caverns that have specific size, shape, and spacing in a cross-sectional view but are infinitely long in the orthogonal direction. In contrast, axisymmetric modeling represents the cavern as a circular opening (in plan view) surrounded by a ring-shaped pillar.

Both types of two-dimensional modeling can represent the stratigraphy (rock layers) and site-specific rock properties. Neither type of two-dimensional modeling can exactly represent the geometry of caverns in a brinefield. The plane-strain model is better for looking at interactions between caverns (effect of cavern spacing and extraction ratio) and the influence of pillar stresses on the cavern roof stability. Axisymmetric modeling is better for looking at specific stress conditions in a cavern roof (cavern span issues) but is not effective for analyzing cavern-spacing issues.

Three-dimensional modeling can accurately represent the geometry of caverns but can be expensive, labor- and computer-intensive, and difficult to visualize the results. Representing the stratigraphy and rock properties using advanced material models is often technically challenging. Three-dimensional modeling, therefore, is usually reserved for specific situations rather than studies of the generic influence of geometrical factors.

As a companion part of this study, BGR performed a series of analyses using two-dimensional modeling (plane strain) to determine when certain aspects of the brinefield geometry become a concern relative to stability of the pillars or cavern roof. In the analyses, the cavern geometry was varied over ranges in the cavern width and the pillar width between caverns for two different cavern heights. The numerical modeling results were analyzed by comparing calculated stresses with a rock failure criterion for rock salt. To account for the long-term strength of rock salt (as compared to salt strength measured in short-term laboratory tests) and to interject a degree of conservatism, only a fraction (30 percent) of the criterion-based rock strength was used to determine the allowable calculated stresses.

Conclusions from the plane-strain modeling were

1. When caverns are considered to be in a row, there is no restriction on the proximity of caverns within the row. In the plane-strain model, the cavern is modeled as infinitely long with no intervening pillars “between caverns.”

2. The required separation between rows (pillar width) depends on the cavern diameter and cavern height. BGR prepared a graph showing the relationship between cavern diameter and the required pillar width for cavern heights of 25 and 40 meters.

Where the conclusions from two-dimensional modeling could not be applied, an alternative analysis method was used. A methodology is described by Van Sambeek [1996; 1998; 1999] for examining the stress magnitudes in salt pillars and the stability of pillars. A modification of this methodology (described in the next section) is used to determine the relative stability of “pillars” isolated by the Akzo Nobel salt caverns. The methodology is also examined to develop a sense of its conservatism relative to the assumptions made and the geometries involved.

2.0 SALT PILLAR EQUATION

Van Sambeek [1996] presents a simple approach to examining the approximate stress state in salt pillars based on numerical modeling results for the limiting cases of axisymmetric and plane-strain to represent the shape of the pillars. For square (or circular) pillars, the ratio of the pillar width (or diameter) to pillar height (W:H) defines the pillar shape. A copy of Van Sambeek [1996] is included as Appendix A. Two later publications [Frayne and Van Sambeek, 1998; Van Sambeek, 1999] extended the salt pillar equation to rectangular-shaped pillars based on three-dimensional numerical modeling results. Copies of these publications are included for reference as Appendix B and Appendix C, respectively.

An important conclusion in the Van Sambeek [1996] paper is that pillar stability can be defined in terms of the ratio between average pillar stresses (expressed as the invariant stresses σ_{eff} and I_1) and a salt-dilation factor (e.g., Van Sambeek et al. [1998]). The equation for calculating the invariant stresses are basically (1) for the average stress in the pillar (sum of the vertical loading stress and twice the horizontal radial stress developed because of the shape of the pillar) and (2) for the shear stress in the pillar resulting from differences in the magnitudes of the principal stresses. Significant from the analysis is that a critical pillar shape exists where stability is indicated, and as the pillar becomes squat, the stability is evermore ensured. Similarly, as a pillar becomes thinner relative to the critical pillar shape, it becomes more prone to dilation and eventually could even fail.

Modified salt-pillar equations were developed specific to the geometry of solution-mined caverns and the stress induced by brine pressure in the cavern. The next section describes the how pillar equations were used to analyze the plane-strain caverns modeled by BGR (the BGR modeling is reported in a companion report.) The purpose of comparing the salt-pillar equations to the BGR modeling results was to test the pillar equations and stability assessment approach as validation for using the equations to assess three-dimensional cavern clusters.

Following the validation of the pillar equations, a methodology was developed that uses the pillar equations to assess the stability of pillars formed by clusters of caverns. In this situation three factors must be accounted for: (1) the extraction ratio within the cavern cluster, (2) the pillar geometry (W:H), and (3) the cavern brine pressure loading that is applied over a portion of the pillar. The methodology provides a set of equations used to determine the allowable height for the pillar for a particular geometrical arrangement of caverns. An example cavern cluster is analyzed and hypothetical conclusions and recommendations given based on those results. Twelve cavern clusters in the Hengelo brinefield were then analyzed to determine the allowable cavern height.

3.0 VALIDATION OF PILLAR-EQUATION APPROACH

The BGR modeled a series of “plane-strain” caverns with ranges of cavern diameter and pillar width. The results from the BGR modeling are now used to validate the RESPEC pillar-equation approach by analyzing the “plane-strain” caverns.

For a plane-strain cavern and pillar situation, the average vertical stress in the pillar next to a cavern is the combination of the vertical stress concentration because of the cavern (geometry effect) and the buoyancy caused by the cavern pressure acting on the cavern roof (pressure effect). The average minor horizontal stress in the pillar, which acts normal to the cavern wall, is a combination of the boundary value (cavern pressure) and geometry-controlled stress that depends on the pillar width-to-height ratio (W:H). The major horizontal stress, which acts along the length of the pillar, is by plane-strain definition exactly equal to the average of the vertical stress and minor horizontal stress; i.e., the deviatoric stress in the direction of the major horizontal stress is exactly zero so there is no creep strain (i.e., the plane-strain stipulation) in that direction. The vertical and two horizontal stresses, respectively, are given by:

$$
\begin{aligned}
\bar{\sigma}_V &= \sigma_0\left(1 + D/W\right) - P\left(D/W\right) \\
\bar{\sigma}_h &= P + \bar{\sigma}_v\left(0.1 \quad W/H\right) \\
\bar{\sigma}_H &= \left(\bar{\sigma}_V + \bar{\sigma}_h\right)/2
\end{aligned}
\tag{3-1}
$$

where:

σ_0 = premining vertical stress

D = cavern diameter

W = pillar width

P = cavern brine pressure

H = cavern height.

These conditions were used in a spreadsheet to calculate the stresses in six caverns involving three cavern diameters at two cavern heights. In the spreadsheet, the required pillar width was calculate to give a stress condition as close as possible to the BGR η = 30 percent criterion. For η = 30 percent in the interval 20 < ($-I_1$) < 50 MPa, $\sqrt{J_2}$ is approximated by $\sqrt{J_2} = 3 + 0.08\ I_1$ so that $\sqrt{J_2}/I_1 = 3/I_1 + 0.08$ (se Figure 3-1).

The BGR, however, found the most critical stress states are in the cavern roof, not in the pillar. Therefore, the critical pillar width calculated with the pillar equation for a particular cavern height and diameter will likely be smaller than that calculated by BGR. The reason is that BGR will specify a larger pillar to reduce the critical stress state in the cavern roof. For that reason, a systematic lowering of the BGR η = 30 percent criterion according to a fixed percentage was used. The RESPEC pillar-equation approach calculated the same size pillars as the BGR plane-strain modeling approach when about 85 percent of the BGR η = 30 percent criterion was used. Simplistically, when the pillar-equation approach is used by applying 85 percent of the η = 30 percent criterion <u>in the pillar</u>, the required pillar size will agree with BGR plane-strain analyses for the η = 30 percent criterion <u>in the roof</u>.

RSI-1477-04-003

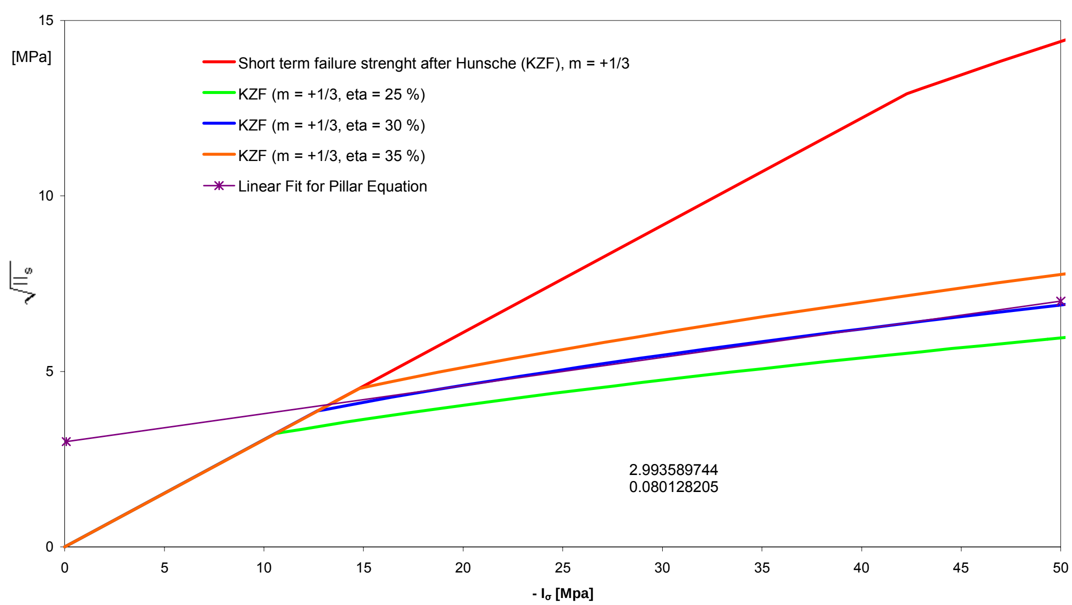

Figure 3-1. Illustration of the Linear Fit Over a Portion of the BGR η = 30 Percent Criterion (for m = +1/3).

The result of the comparison for three combinations of cavern diameter and cavern height is given in Table 3-1.

As suggested above, the pillar equation approach requires the similar-sized pillar as the BGR approach for the range of cavern diameters if 85 percent of the η = 30 percent criterion is used to calculate the critical stresses in the pillar equation. The technical reason for a greater pillar width in the BGR plane-strain analyses probably relates to the span of the cavern roof relative to a fixed stratigraphy; i.e., thickness of salt in the roof and flexure of the span with its resultant stress conditions near the roof/cavern-wall intersection.

The conclusion from this comparison is that the pillar equation is validated for determining the minimum pillar dimension so long as a somewhat more conservative long-term failure criterion is used. The pillar-equation approach will now be extended to axisymmetric pillars in cavern clusters based on the same assumptions.

Table 3-1. Comparison of Required Pillar Diameter for BGR and Pillar Equation Approaches

Cavern Height (m)	Cavern Diameter (m)	BGR Required Pillar Diameter (m)	Pillar Equation Required Diameter (m)	Ratio (%)
25	50	29.7	31.5	94.3
25	100	51.8	51.2	101.3
25	150	70.5	68.0	103.7
40	50	33.2	35.5	93.5
40	100	58.7	59.3	99.0
40	150	80.8	80.2	100.7

4.0 CAVERN CLUSTER ANALYSIS

For a cavern cluster, the following methodology was used to determine the adequacy of the pillar within the cluster:

Step 1. Inscribe a circular pillar that has at least three points of tangency with surrounding caverns. Measure the diameter, W.

Step 2. Draw two rays from the center of the inscribed circular pillar to points of tangency on either side of *each* cavern.

Step 3. Measure the angle between each pair of rays (where a cavern sits within the pair of rays.

Step 4. Sum the measured angles to determine the total angle, β. Let $\gamma = \beta/360$.

Step 5. Over scribe another circle using the same center as in Step 1 where this circle passes through as many as possible of the points of tangency between rays and caverns. Measure the diameter, W_0

Step 6. Calculate the three average principal stresses according to:

$$\begin{aligned}
\bar{\sigma}_V &= \sigma_0 \frac{A_T}{A_P} - P\frac{A_{cav}}{A_P} \\
&= \sigma_0 \left[\frac{W_0^2}{W_0^2 - \gamma\left(W_0^2 - W^2\right)}\right] - P\left[\frac{\gamma\left(W_0^2 - W^2\right)}{W_0^2 - \gamma\left(W_0^2 - W^2\right)}\right] \qquad (4\text{-}1) \\
&= \frac{\sigma_0 - P\gamma\left(1 - \left(W/W_0\right)^2\right)}{1 - \gamma\left(1 - \left(W/W_0\right)^2\right)}
\end{aligned}$$

If $\sigma_0 \approx 2P$

$$\bar{\sigma}_V = P\left[\frac{2 - \gamma\left(1 - \left(W/W_0\right)^2\right)}{1 - \gamma\left(1 - \left(W/W_0\right)^2\right)}\right]$$

$$\bar{\sigma}_r = \gamma\left[P + 0.1\bar{\sigma}_V\left(\frac{W}{H}\right)\right] + (1-\gamma)\sigma_0 \tag{4-2}$$

$$\bar{\sigma}_\theta = 0.1\bar{\sigma}_V\left(\frac{W}{H}\right) \tag{4-3}$$

where:

- P = cavern brine pressure = 5.25 MPa
- H = cavern height
- W = inscribed circular pillar diameter, A_P is the area of the pillar
- W_0 = over scribed circular pillar diameter, A_T is the area of the over scribed pillar including part of the caverns, A_{cav} is only the cavern area in the over scribed circular pillar
- γ = (cumulative angle of cavern exposure)/360
- σ_0 = premining stress state
- $\bar{\sigma}_V$ = average vertical stress within the inscribed pillar area accounting for the caverns and brine pressure
- $\bar{\sigma}_r$ = average radial stress developed between the cavern edge (σ_r = P) and the center of the inscribed pillar, subject to $\bar{\sigma}_r \leq \bar{\sigma}_V$
- $\bar{\sigma}_\theta$ = average tangential stress developed in the inscribed pillar.

Step 7. Calculate two stress invariants used to quantify stability:

$$\sqrt{J_2} = \sqrt{\frac{1}{6}\left[\left(\bar{\sigma}_V - \bar{\sigma}_r\right)^2 + \left(\bar{\sigma}_r - \bar{\sigma}_\theta\right)^2 + \left(\bar{\sigma}_\theta - \bar{\sigma}_V\right)^2\right]} \tag{4-4}$$

$$I_1 = \bar{\sigma}_V + \bar{\sigma}_r + \bar{\sigma}_\theta \tag{4-5}$$

Step 8. Calculate $\xi = \sqrt{J_2}/I_1$.

Step 9. Compare $\xi = \sqrt{J_2}/I_1$ at 85 percent of η = 30 percent for this I_1:

$$\xi_{\eta=30\%} = \left(\frac{3}{I_1} + 0.08\right)(85\%) \qquad 20 \leq I_1 \leq 40 \tag{4-6}$$

Step 10. If ξ from Step 8 is less than $\xi_{\eta=30\%}$, then cluster pillar is stable; otherwise unstable.

Step 11. Calculate the maximum stable cavern height by using a root solver for H to achieve $\xi = \xi_{\eta=30\%}$.

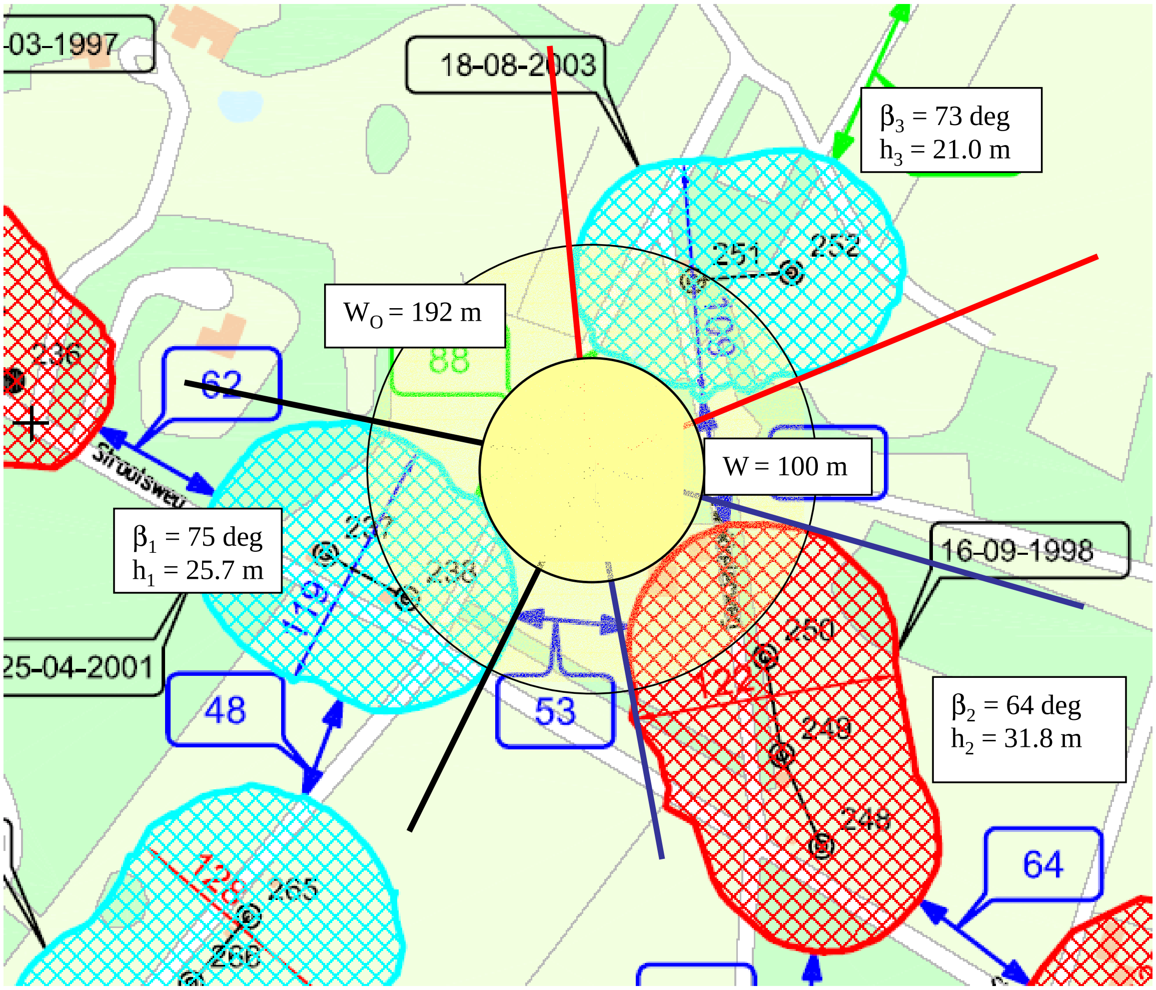

Cavern Brine Pressure	P	5.25 MPa				
Inscribed Pillar Diameter	W	100 m				
Overscribed Pillar Diameter	Wo	192 m				
Cumulative Cavern Angle	β	212 degrees				
Stability Criterion	A	3				
$\sqrt{J_2} / I_1 = (A/I_1 + B)*C$	B	0.08				
	C	85%				
Calculated Stresses	σ_V	σ_r	σ_θ	$\sqrt{J_2}$	I_1	$\sqrt{J_2} / I_1$
	14.45	10.52	5.27	4.61	30.23	0.152
Allowable Pillar Height to Meet Stability Criterion	h_{max}	27.43 m				

Figure 4-1. Example of Cavern-Cluster Pillar Analysis With Calculated Allowable Pillar Height.

This methodology is illustrated in Figure 4-1 for a pillar in a cluster of caverns 237-248-251. The inscribed pillar has a diameter (W) of 100 meters and the over scribed pillar has a diameter (W_0) of 192 meters. The three caverns define the three angles (β_1, β_2, and β_3) with magnitudes of 75, 64, and 73 degrees, respectively, for a total angle of 212 degrees. The principal stresses for this situation are calculated in a spreadsheet based on the equations listed above. For the stresses shown, a root solver was used to determine the cavern height (h_{max}) that would cause $\sqrt{J_2}/I_1 = 3/I_1 + 0.08$, including an 85 percent reduction in the allowable stress condition.

For the cavern cluster in the example, the calculated maximum cavern height for the current cavern sizes and locations is 27.4 meters. The current cavern heights (h_1, h_2, and h_3) are 25.7, 31.8 (inactive), and 21.0 meters, respectively. The height of cavern 248; therefore, already exceeds the allowable height. Mining should remain stopped in Cavern 248, but mining could hypothetically continue in Caverns 237 and 251 until their heights reach the critical height (27.4 meters).

The pillar-equation approach was used to assess cavern clusters identified by Akzo Nobel, State Supervision of Mines, or RESPEC, and the results are summarized in Table 4-1.

Table 4-1. Analysis – Parameter Values and Calculated Maximum Cavern Height for 12 Cavern Clusters

Cavern Cluster	Caverns Involved in Cluster			W (m)	W_o (m)	β (deg)	h_{max} (m)
1	239	248	270	80	169	236	20.3
2	201	305	308	124	256	193	34.6
3	237	248	251	101	204	214	27.2
4	182	198	352	108	218	196	30.1
5	314	317	325	124	218	159	37.9
6	237	248	265	134	254	201	37.7
7	275	278	287	125	232	179	36.7
8	275	278	290	146	264	172	43.6
9	225	314	331	114	240	213	30.4
10	207	259	261	111	210	189	31.9
11	393	396	402	126	240	161	37.8
12	402	405	414	111	218	150	33.7

5.0 Reliability of the Method

The pillar equations are intended for salt pillars in a dry mine. That is, a mass of salt with fully isolated vertical surfaces (pillar ribs), where the mass of salt sits between the exposed roof and floor of the mine, and air pressure acts on all exposed surfaces. By definition, the horizontal stress magnitude at the edges of the pillar is zero (neglecting atmospheric pressure). All around the pillar, the horizontal stress increases from zero either to a maximum value at the center of the pillar or to a maximum value that remains constant across the core of the pillar. For tall, thin pillars the maximum value is low; for short, squat pillars the maximum value might be the original (premining) horizontal stress or even be greater for large average vertical stress concentrations. The vertical stress can have vastly different distributions that depend on the size and shape of the pillar and can not be easily generalized. Regardless of the distribution, the vertical stress will have an average value for the vertical stress that depends on the vicinity extraction ratio and the support provided by surrounding pillars and unmined salt.

The situation in a solution-mine field is much different than an underground dry salt mine. The prominent differences, however, interject conservatism into the conclusions drawn from use of the pillar equations. Aspects that are different between dry- and solution-mining, and why conservatism results, include:

1. Pillars between caverns are not fully isolated; therefore, the horizontal stress at the edge of the imaginary circular pillar is not zero, and in some portions of the pillar "edge" could have a magnitude as high as the pre-mining horizontal stress.
2. Portions of the pillar edge exposed to the cavern brine are subjected to a brine pressure loading; hence, the horizontal stress across the pillar does not increase from zero, but rather increases from the brine pressure value.
3. The pillar height is taken from the "tallest" cavern in the cluster. If the other caverns are shorter, the portion of the pillar next to those caverns will be more stable.

Each of these interjects conservatism (or an incremental factor-of-safety).

Aspects do exist where one can argue that the brine-filled caverns might invalidate the pillar-equation approach. These include:

1. The brine from the cavern could infiltrate the surrounding salt and weaken it and invalidate the basis of the equations.
2. The edges of the cavern could deteriorate and cause an enlargement of the cavern diameter.

3. The cavern roof could fail (cavern migration) despite the adequacy of the pillars to support the overburden.

The aspect of brine infiltration is not expected because the brine cavern is not pressurized above that of a static brine column to surface. The brine pressure is never expected to exceed 50 percent of the lithostatic rock stress (i.e., about 0.012 MPa/m depth for the brine pressure compared to 0.025 MPa/m for the rock stress). Research results reported by the Solution Mining Research Institute indicate brine infiltration is not likely until the ratio between the brine pressure and the lithostatic stress exceeds at least 90 percent.

Repeated sonar surveys of actual caverns have not detected deterioration of the edges of caverns. For the most part, cavern profiles indicate a constant cavern diameter or systematic diameter growth as a consequence of continuing solution mining. If cavern edge deterioration were excessive, it would have been noted in past surveys.

Cavern migration by progressive roof failure has and may still be occurring for several caverns. Cavern migration is believed to relate more to absence of a salt roof above the cavern than to the support capability of the surrounding salt "pillar."

Over and above the reasoning that the pillar design equations are conservative, additional conservatism is interjected by the failure criterion for the salt. In these analyses, only 30 percent of the measured "short-term" salt strength was used to help ensure that an appropriate long-term strength parameter was applied.

6.0 CONCLUSIONS AND RECOMMENDATIONS

A methodology was developed to assess the stability of cavern clusters. Twelve clusters were analyzed and conclusions and recommendations for each cluster are as follows.

Cluster 1: Each of the three caverns has a height that exceeds the maximum allowable height for the pillar inscribed within the cavern cluster. Before this analysis, two caverns were already inactive (Caverns 239 and 248); mining has since been stopped in the third (Cavern 270).

Cluster 2: Two of the caverns may have heights that exceed the allowable height; Cavern 201 is inactive and Cavern 305 must be stopped. Cavern 308 can continue to be mined until the height reaches the allowable height of 34.6 m.

Cluster 3: Inactive Cavern 248 exceeds the allowable height. Caverns 237 and 251 have heights less than the allowable. Cavern 237 is at the intersection of two lines of caverns. Mining in Cavern 237 will be stopped, because of BGR criteria for caverns in lines. Mining can continue in Cavern 251 until its height reaches the allowable 27 m.

Cluster 4: Each of the three caverns is below the allowable height. Caverns 182 and 198 are inactive. Continue mining in Cavern 352 up to an allowable height of 30 m.

Cluster 5: Each of the three caverns is below the allowable height. Mining can continue in Caverns 317 and 325 up to the allowable height of 38 m. Cavern 314 is also in Cluster 9 where the allowable height is restricted to 30 m.

Cluster 6: Each of the three caverns is below the allowable height. Cavern 248 is already inactive. Mining could continue in Caverns 237 and 265 relative to this methodology; however, Cavern 237 is at the intersection of two lines of caverns. Mining in Cavern 237 will be stopped because of BGR criteria for caverns in lines. Mining can continue in Cavern 265 until its height reaches the allowable 37 m.

Cluster 7: Each of the three caverns is below the allowable height. Mining could continue in all three caverns relative to this methodology. Caverns 275 and 287 are poorly positioned according to the BGR criteria for lines of caverns, and mining in Caverns 275 and 287 will be stopped. Mining in Cavern 278 can continue up to 37 m.

Cluster 8: This cluster contains two of the same caverns as Cluster 7 – Caverns 275 and 278. Each of the three caverns is below the allowable height. Cavern 275 will be shut down based on the BGR criteria for caverns in a line. Mining can continue in Cavern 278 up to a height of 37 m (see Cluster 7). Mining of Cavern 290 can continue until it reaches an allowable height of 43.7 m.

Cluster 9: Inactive Cavern 225 exceeds the allowable height of 30.4 m. Caverns 314 and 331 less than the allowable height, and mining can continue until their heights reach 30 m.

Cluster 10: Inactive Cavern 259 is nominally at the allowable height of 31.9 m. Caverns 207 and 261 have heights considerably less than the allowable height, and mining can continue until their heights reach at least 30 m.

Cluster 11: Based on the assumed future cavern expansion and remaining pillar diameter, the caverns all have heights well below the allowable and mining could conceivably continue until their heights exceed 36 m. Cavern 402 is poorly positioned, however, based on the BGR criteria for caverns in a line. Mining will be stopped in Cavern 402.

Cluster 12: As with Cluster 11, these caverns are poorly positioned. The future pillar diameter is generously estimated to be 111 m, which gives an allowable height for the caverns of about 34 m. Cavern 402 is to be stopped (see Cluster 11). Therefore, mining Caverns 405 and 411 can continue to an allowable height of 34 m. If the cavern expansion is greater than that illustrated for Cluster 12 in Appendix D, then the allowable height should be reassessed.

7.0 REFERENCES

BGR, 1998. *Rock-Mechanical Expertise Concerning the Stability of the Existing Caverns and for Dimensioning of New Caverns in the Hengelo Field*, report (English Translation) prepared by Bundesanstalt Fur Geowissenschaften und Rohstoffe (BGR), Hanover, Germany, for Akzo Nobel Salt, Hengelo, The Netherlands.

Frayne, M. A. and L. L. Van Sambeek, 1999. "Three-Dimensional Verification of Salt Pillar Design Equation," *Proceedings, Fifth Conference on The Mechanical Behavior of Salt,* University of Bucharest, Bucharest, Romania, August 9–11, N. D. Cristescu; J. R. Hardy, Jr.; and R. O. Simionescu (eds.) A. A. Balkema, Netherlands, 2002, pp. 405–409.

Van Sambeek, L. L., 1996. "Salt Pillar Design Equation," *Proceedings, Fourth Conference of the Mechanical Behavior of Salt*, École Polytechnique de Montréal Mineral Engineering Department, Quebéc, Canada, June 17 and 18, M. Aubertin and H. R. Hardy, Jr. (eds.), Penn State University, Trans Tech Publications, Clausthal, Germany, 1998, pp. 495-508.

Van Sambeek, L. L., 1999. *Revised 3D Salt Pillar Equations – Power Law Form*, RESPEC Internal Document, November 3.

APPENDIX A

PILLAR ANALYSES PARAMETERS FOR THE 12 CAVERN CLUSTERS LISTED IN TABLE 4-1

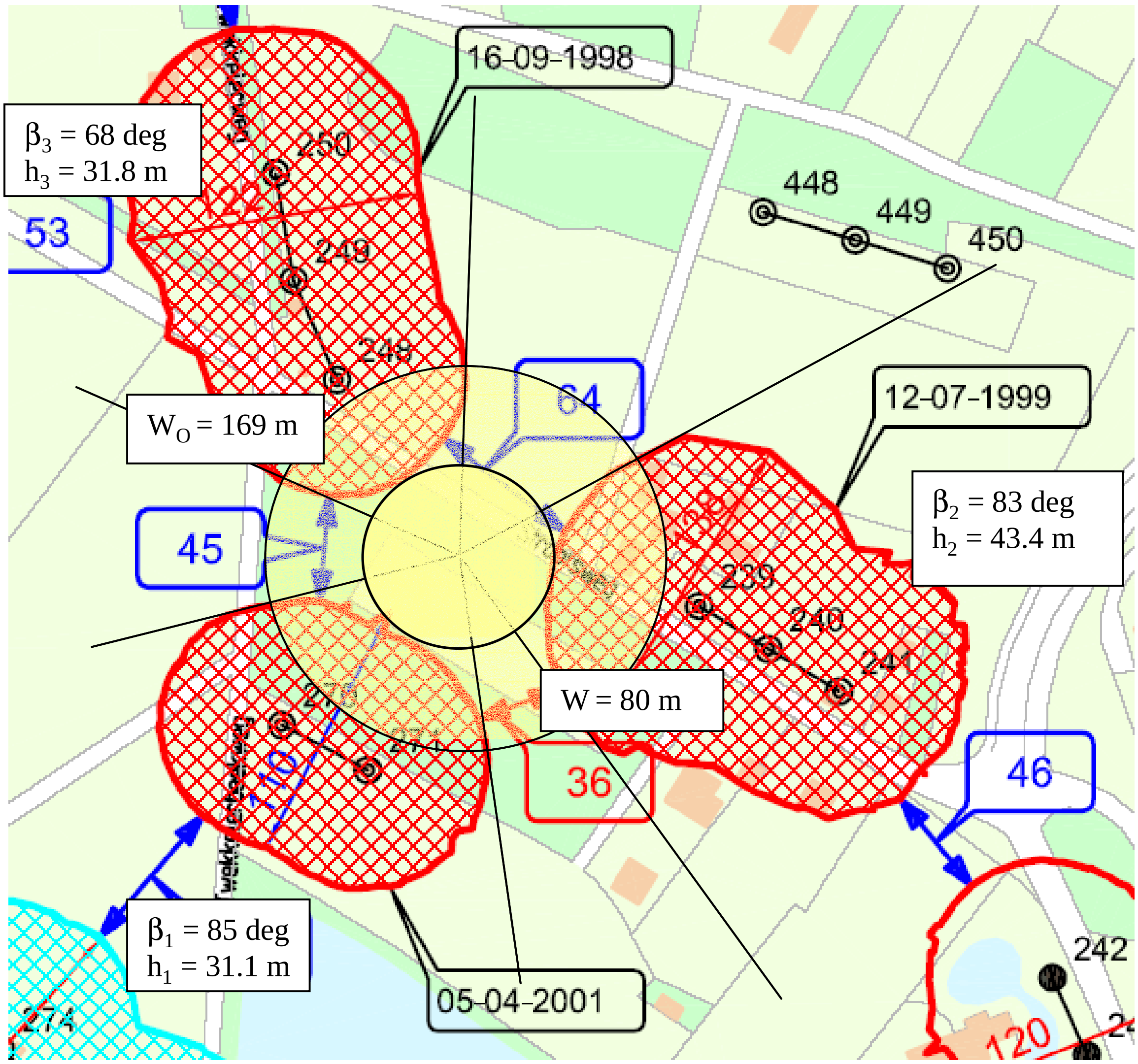

Cavern Cluster 1

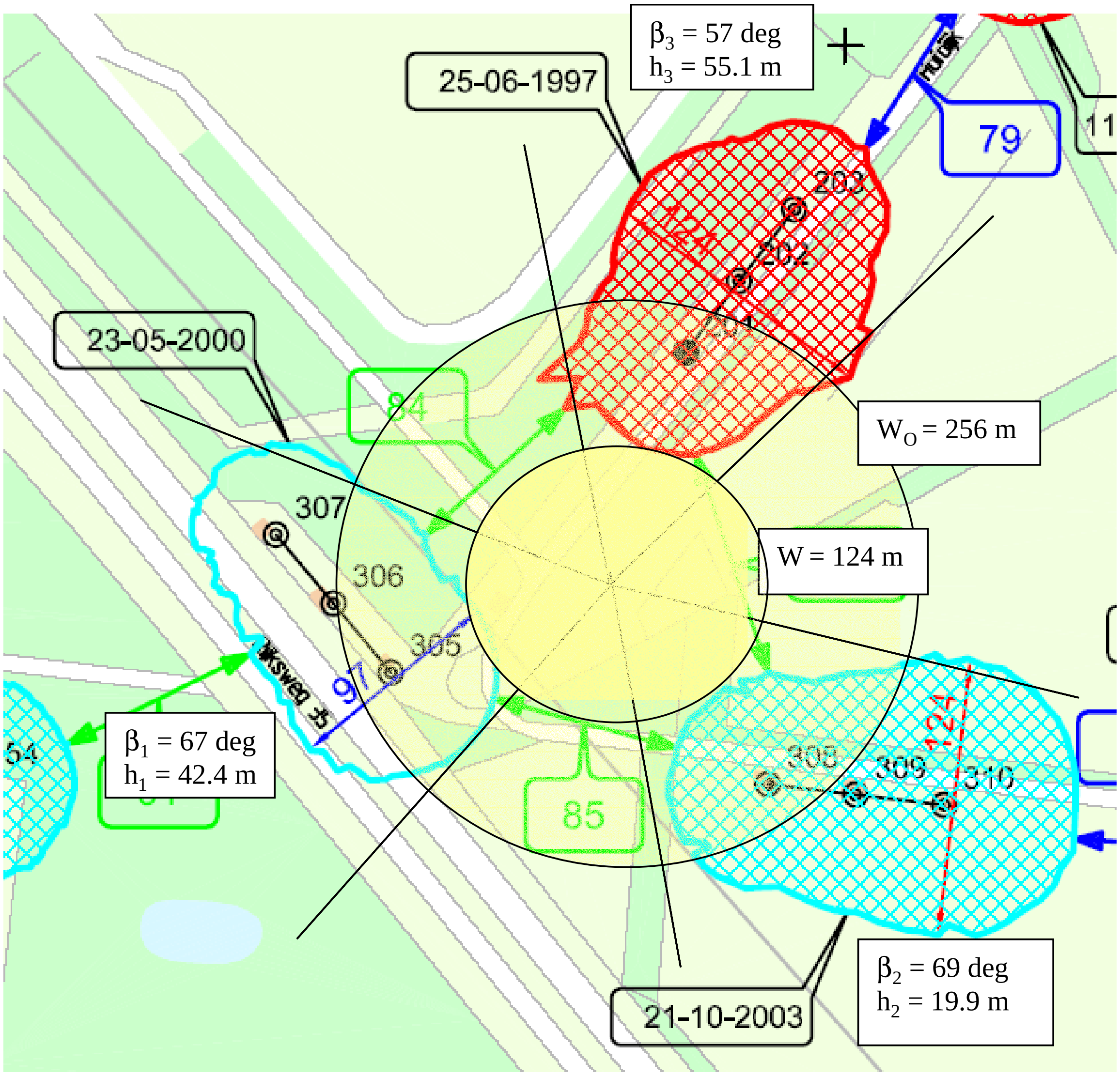

Cavern Cluster 2

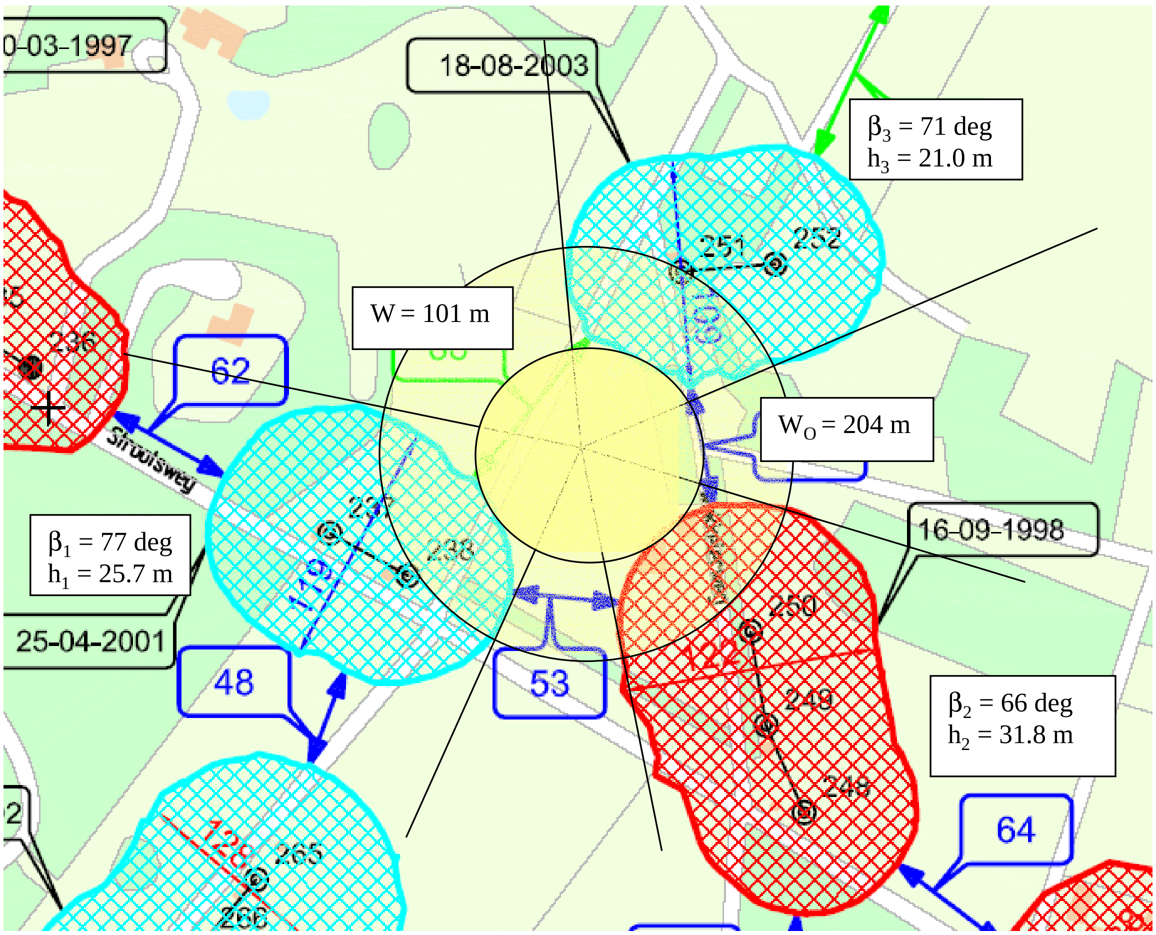

Cavern Cluster 3

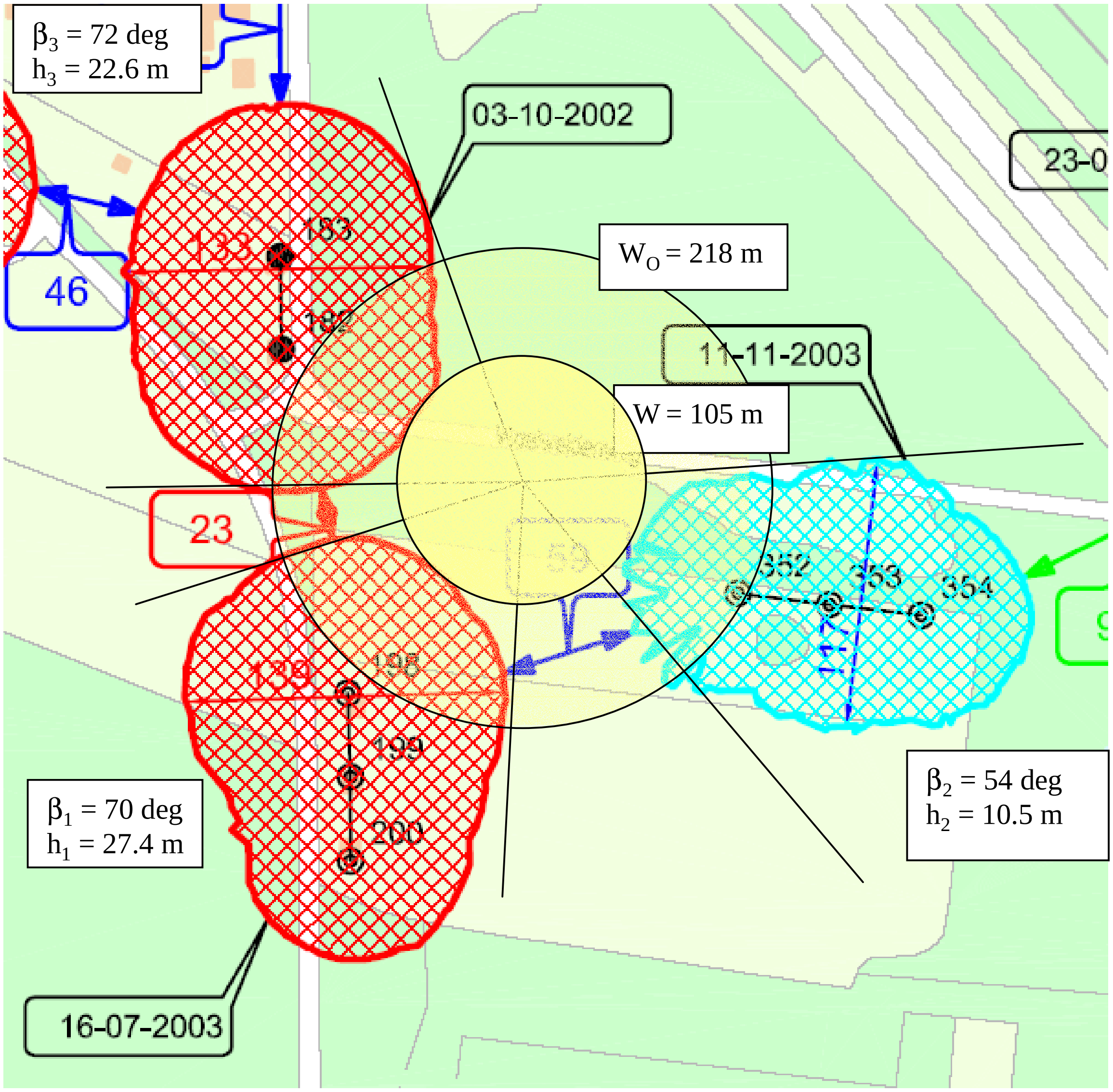

Cavern Cluster 4

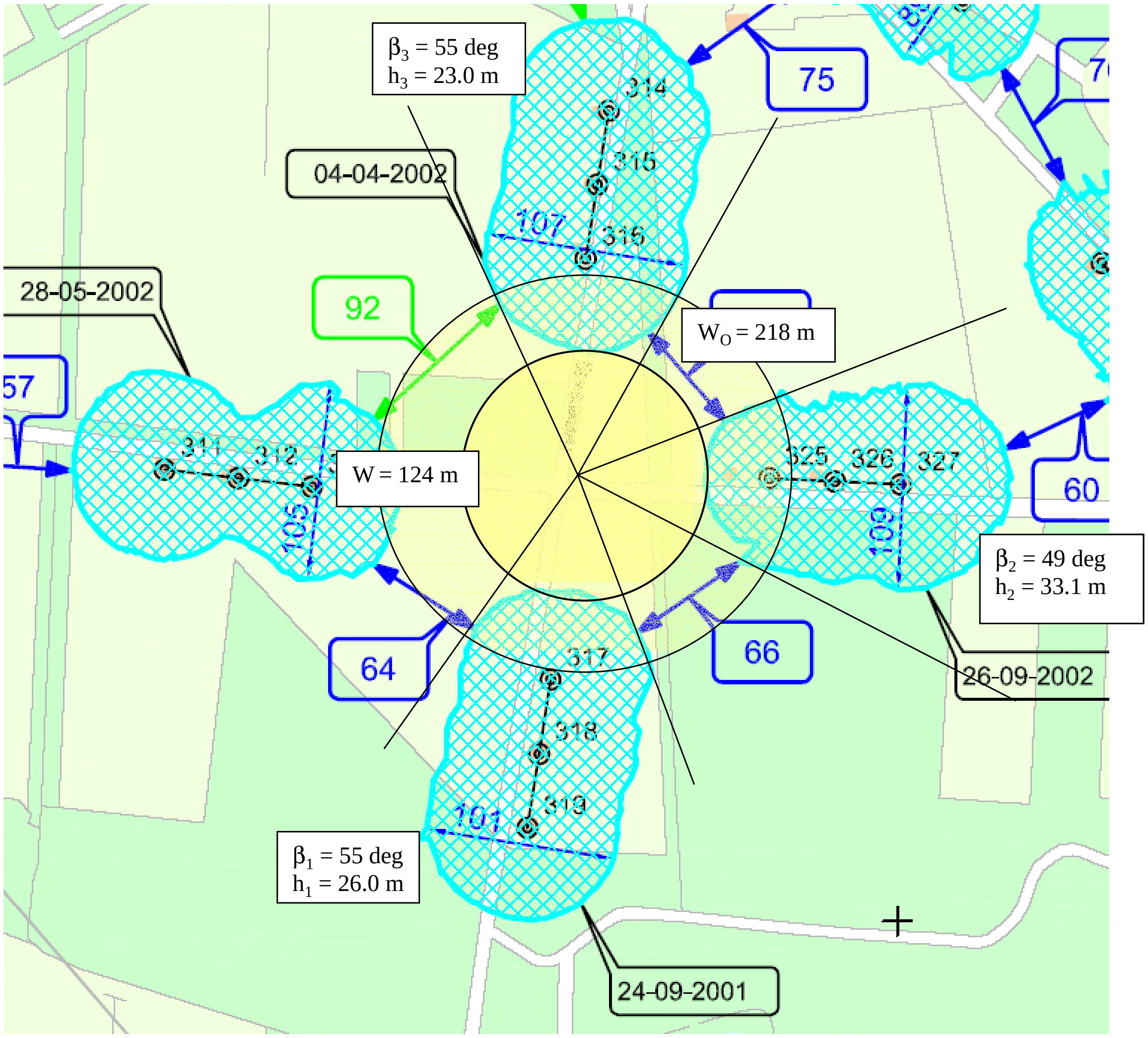

Cavern Cluster 5

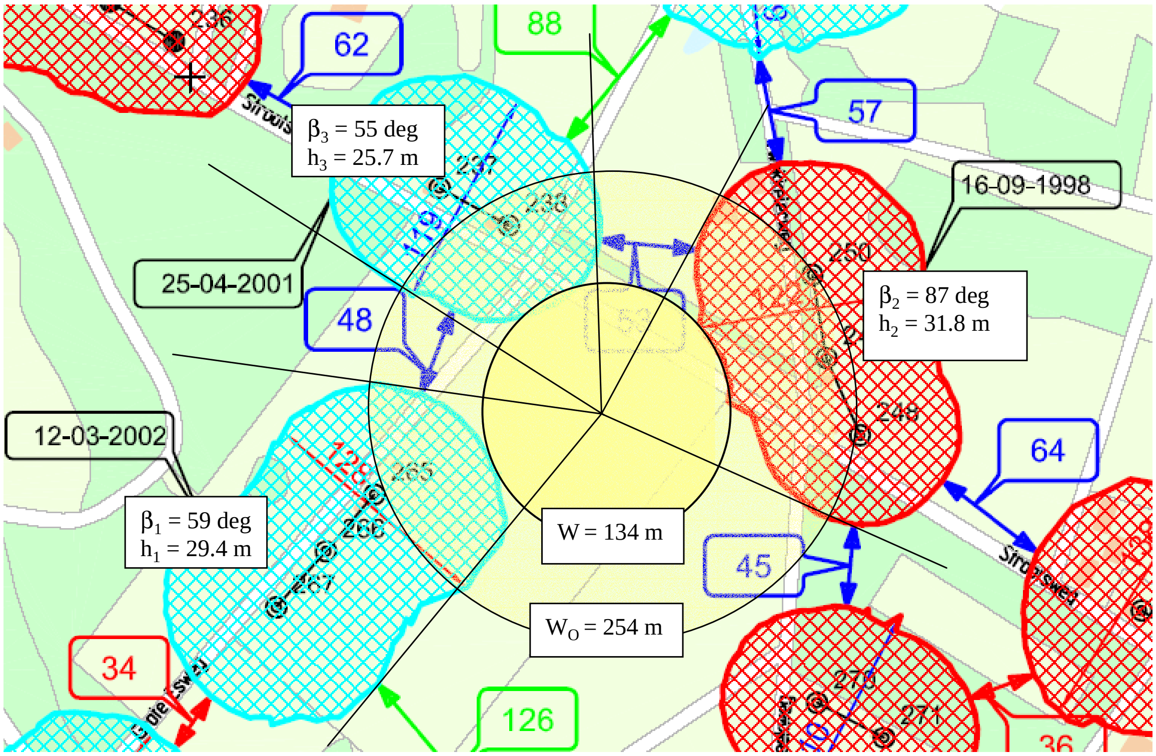

Cavern Cluster 6

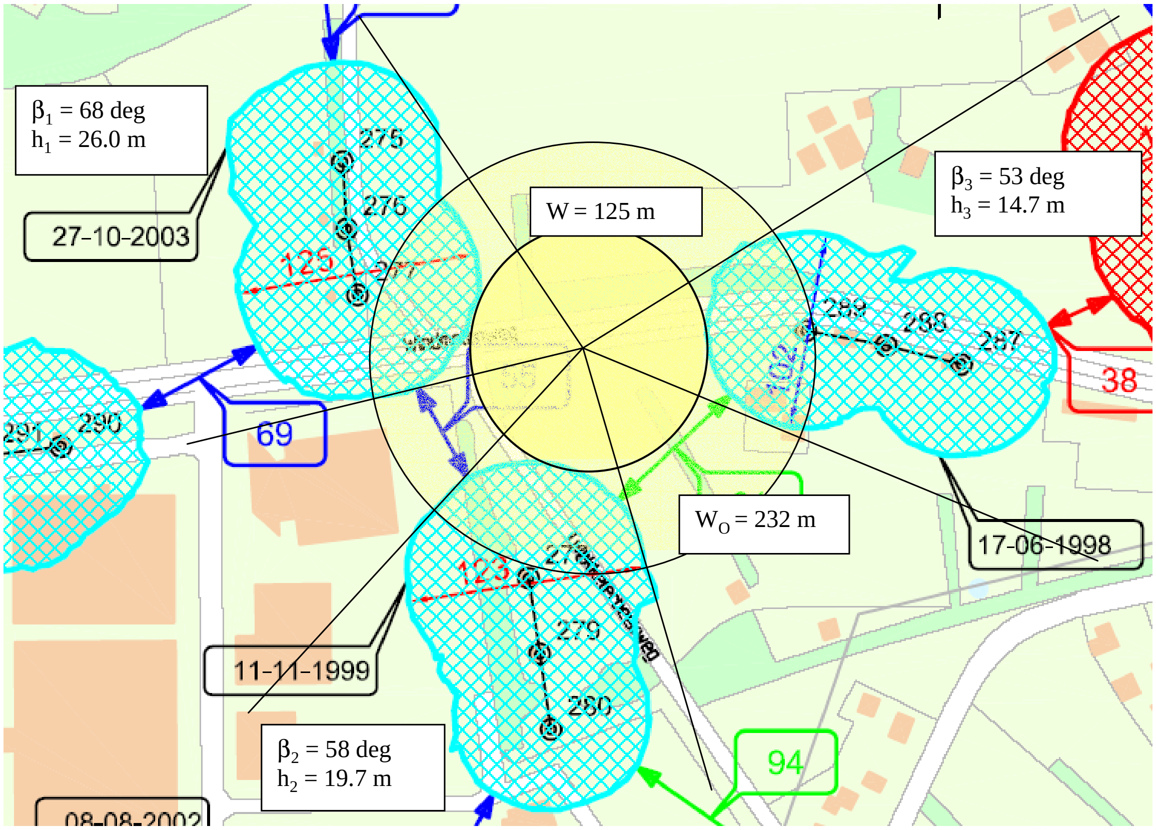

Cavern Cluster 7

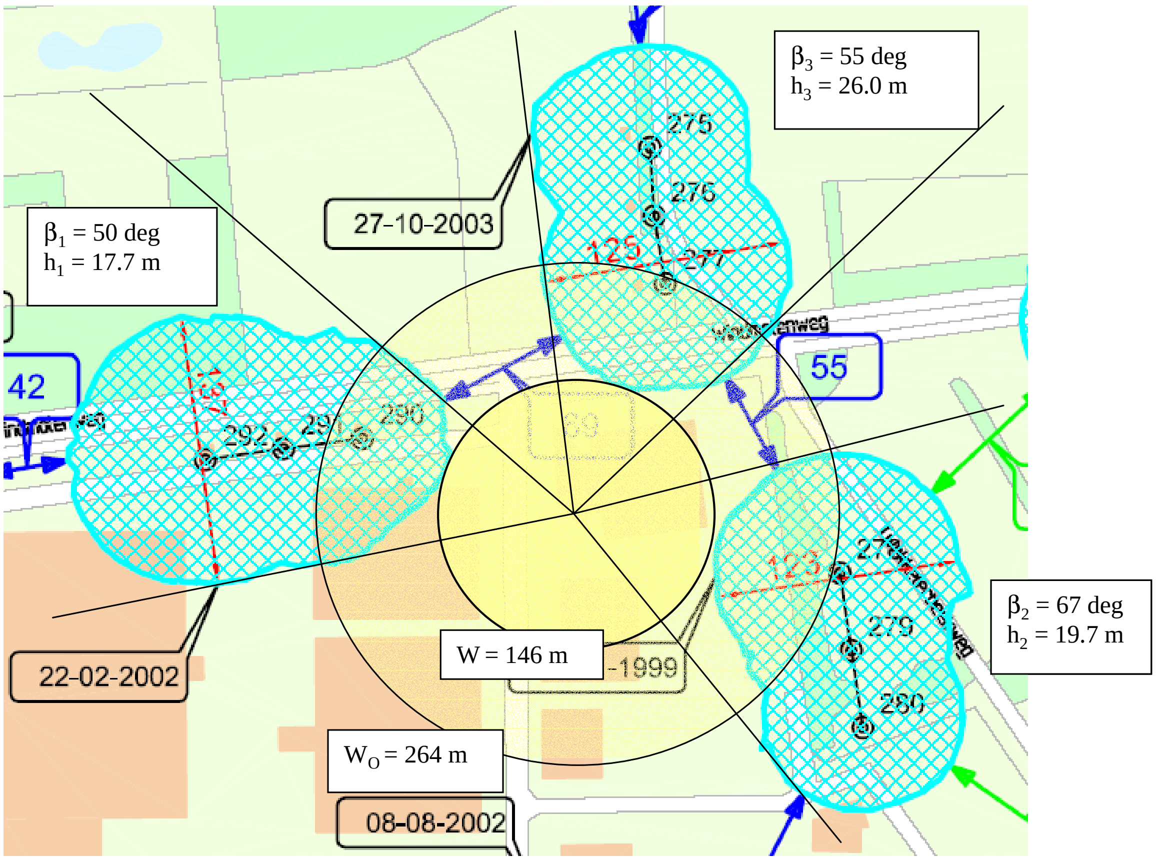

Cavern Cluster 8

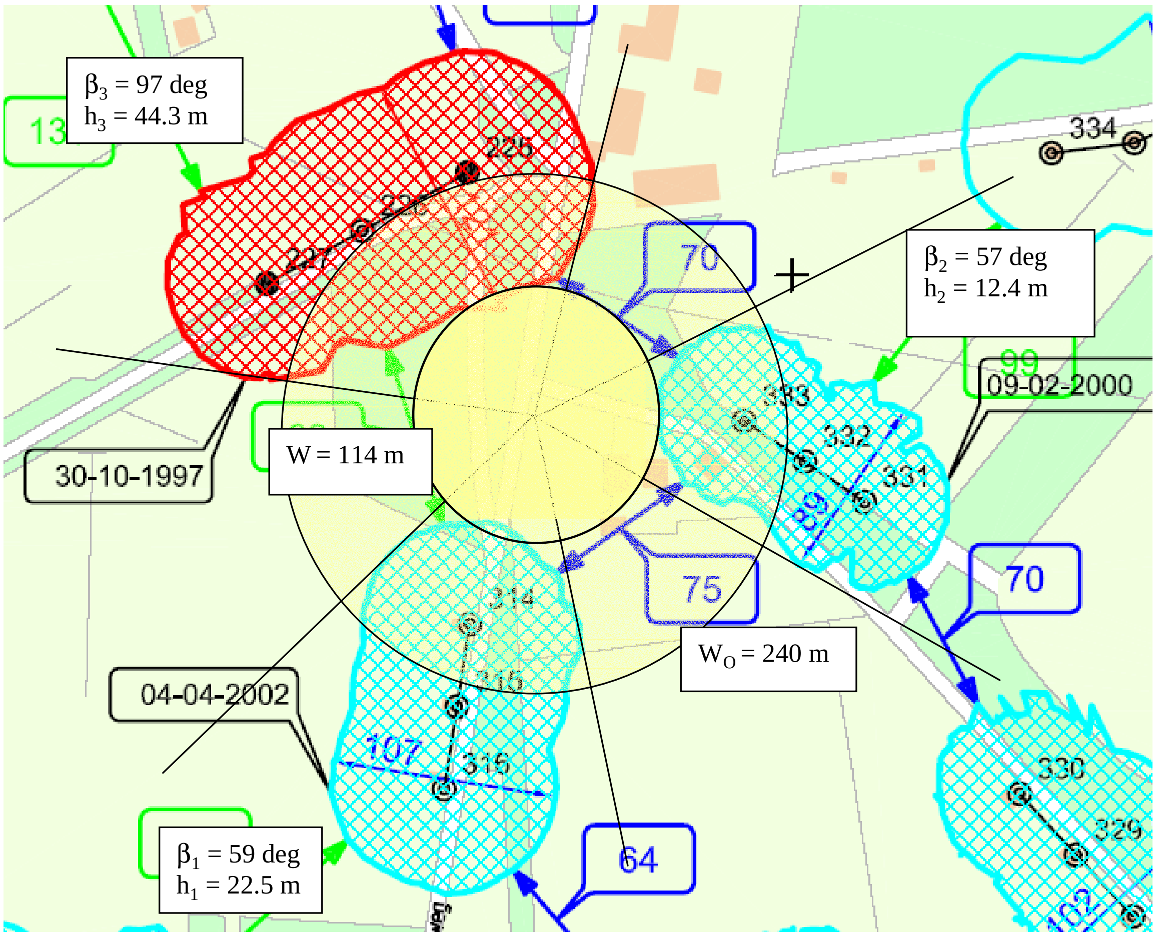

Cavern Cluster 9

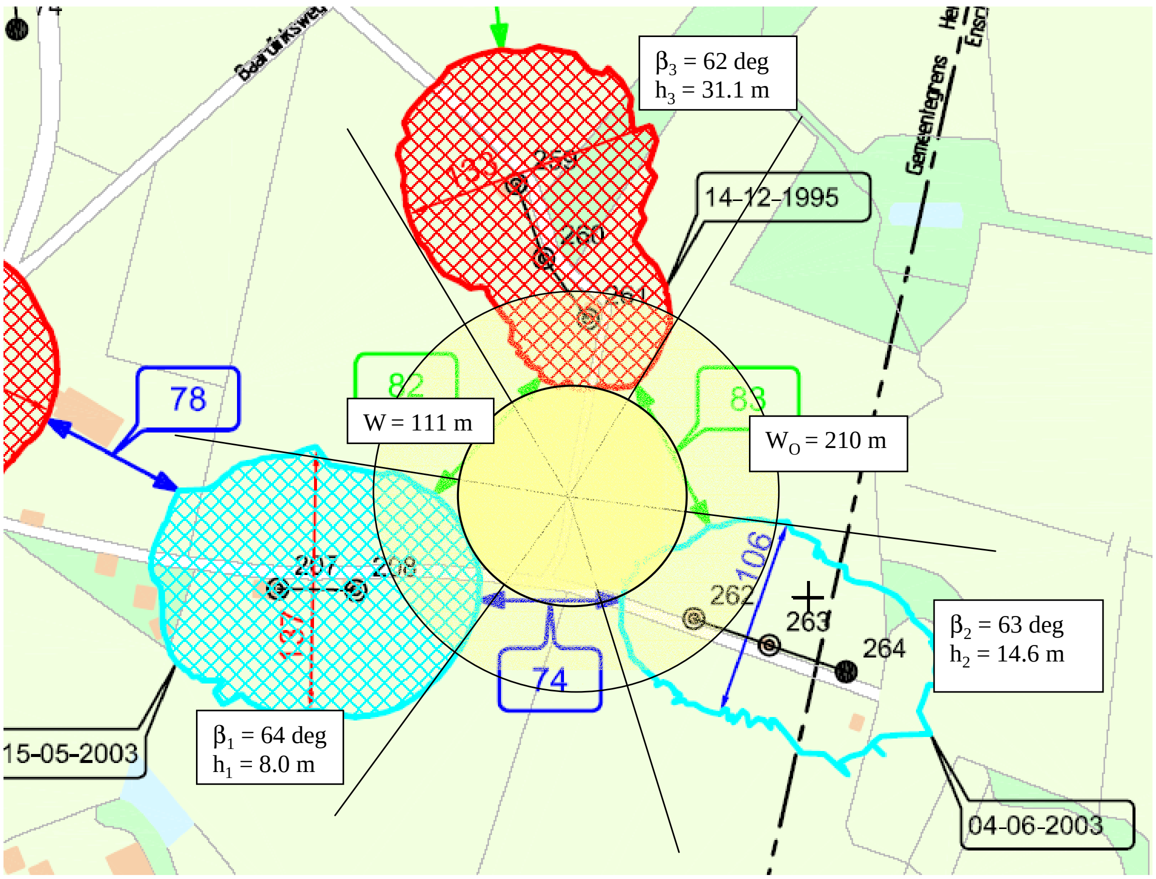

Cavern Cluster 10

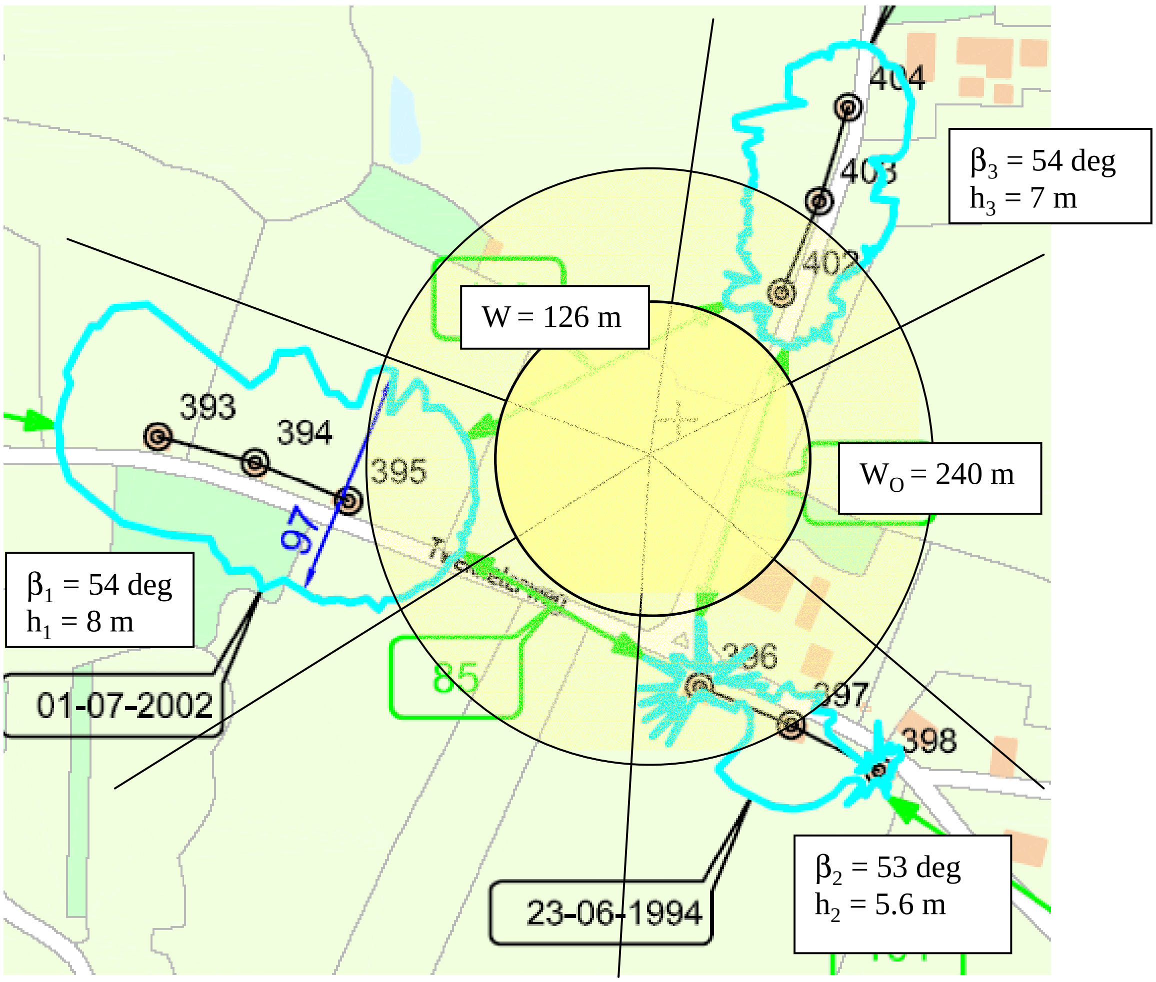

Cavern Cluster 11

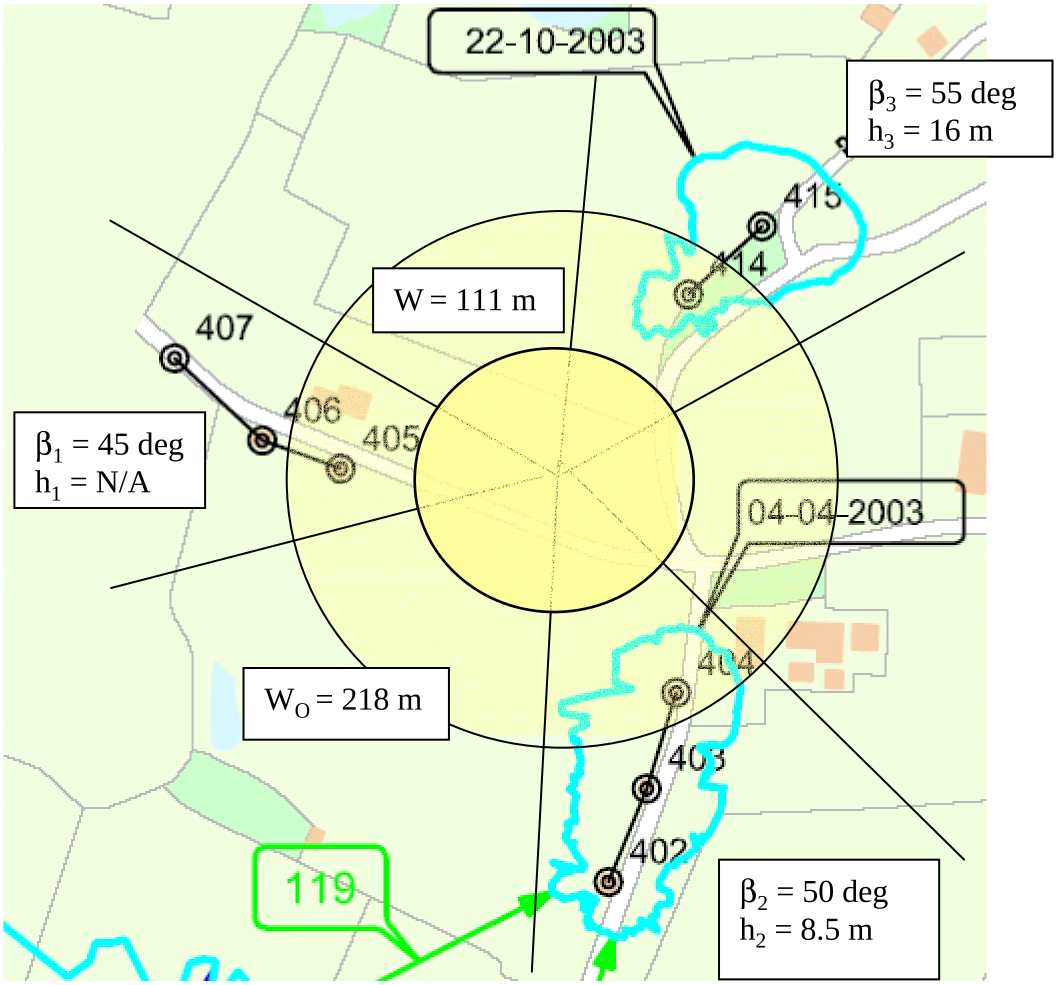

Cavern Cluster 12

APPENDIX B

SALT PILLAR DESIGN EQUATION

SALT PILLAR DESIGN EQUATION

5.1.2.e

RE/SPEC Inc., Rapid City, SD 57701

ABSTRACT

Specification of properly sized pillars to support the overburden is one of the most challenging aspects of salt mine design. A series of numerical modeling analyses shows that a simple pillar design equation for salt pillars adequately reproduces results of extensive modeling efforts. This paper describes (1) the basis for the pillar design equation, (2) equation verification by comparison with numerical modeling results, and (3) equation validation by comparison with measurements and observations of salt-pillar behavior.

INTRODUCTION

Because ore left in pillars detracts from the utilization of the mineral resource, the size of pillars can influence the viability of an underground mine. Even for salt (and potash) mines, where the mineral resource is often extensive, pillar design is still important because pillar size influence rates of closure underground (equipment clearance and headroom), rates of subsidence on the surface, and life of the mine. Laboratory creep testing of salt specimens to obtain sophisticated creep laws and recent developments in numerical modeling have allowed rock mechanics practitioners to examine expected deformation patterns and rates in salt pillars. In particular, numerical modeling provides insight about time-dependent stress states in pillars and the surrounding rock, as the process of creep redistributes stresses. While elegant in its purpose, numerical modeling can, however, be cumbersome in practice. A series of numerical modeling analyses demonstrates that a simple pillar design equation for salt pillars is capable of reproducing the results of extensive modeling efforts. This equation simplifies comparisons of different pillar sizes and shapes, and provides a tool for estimating stress conditions in salt pillars when deformation data are available.

 5.1.2.e

BACKGROUND

Average Vertical Pillar Stress

The removal of material in an underground mine causes a redistribution of the stresses from the mined area onto pillars or adjacent unmined areas. Stress redistribution (concentration) can be defined by the tributary loading theory with modification to account for special geometrical conditions (e.g., arching across narrow panels). According to tributary loading theory and for a competent pillar, the average vertical stress in a pillar is equal to the weight of the overburden borne by the pillar divided by the load-bearing area of the pillar. Hence, the average vertical stress is:

$$\overline{\sigma}_v = W_{OB}/A_p = \gamma\, z/(1 - E) \tag{1}$$

where:

W_{OB} = weight of overburden

A_p = pillar area

E = areal extraction ratio

z = overburden thickness (i.e., depth)

γ = average stress gradient for the overburden.

For mines with a wide expanse, $\overline{\sigma}_v$ is applicable for most pillars. For narrow mines, or narrow panels within a mine, $\overline{\sigma}_v$ may be reduced by a geometrical factor, but an average vertical stress still exists; i.e.,

$$\overline{\sigma}_v = \alpha\left[\gamma\, z/(1 - E)\right] \tag{2}$$

where α = geometrical factor $0 < \alpha \leq 1$. The geometrical factor is not used further in this paper; for the rest of the paper, $\alpha = 1$, which implies full overburden loading as occurs in wide mines and panels.

According to tributary loading (Equation 1), the average vertical stress depends neither on the size nor the shape of pillars (assuming pillars are competent). The stresses acting normal to the vertical stress — the horizontal stresses — have significant pillar-shape dependencies, however.

Average Horizontal Stresses

Van Sambeek [1984] proposes that the average horizontal stresses in a rectangular-shaped salt pillar after stress-relief creep (at steady-state stress conditions) are:

$$\overline{\sigma}_h = \overline{\sigma}_v \left(0.1 \ W_h{:}H\right)$$
$$\overline{\sigma}_H = \overline{\sigma}_v \left(0.1 \ W_H{:}H\right) \tag{3}$$

where:

$\overline{\sigma}_h$, $\overline{\sigma}_H$ = average horizontal stress parallel to shortest and longest pillar dimensions

W_h, W_H = shortest and longest horizontal pillar dimensions

H = pillar height (vertical dimension).

A logical limit on the magnitude of the average horizontal stresses is that they do not exceed the average vertical stress. Therefore, application of Equation 3 is restricted to W:H < 10; later it will be shown that W:H < 5 is a better limit.

Average Effective Stress

The von Mises effective stress measure is commonly used to determine the creep rate for salt. The von Mises effective stress, when expressed in terms of the principal stresses, is:

$$\sigma_{ef} = \sqrt{3J_2} = \sqrt{\left\{\left(\sigma_1 - \sigma_2\right)^2 + \left(\sigma_2 - \sigma_3\right)^2 + \left(\sigma_3 - \sigma_1\right)^2\right\}/2} \tag{4}$$

If assumptions are made that (1) the average effective stress for rectangular-shaped pillars can be calculated from average vertical and horizontal stresses and (2) the vertical and horizontal stresses are principal stresses, and for simplification, $W_H = \beta W_h$ and $W = W_h$, then:

$$\overline{\sigma}_h = \overline{\sigma}_v \left(0.1 \ W{:}H\right) \quad \text{and} \quad \overline{\sigma}_H = \overline{\sigma}_v \left(0.1\beta \ W{:}H\right) \tag{5}$$

and:

$$\left(\overline{\sigma}_{ef}\right)_\beta = \overline{\sigma}_v \sqrt{\left(0.1 \ W{:}H\right)^2 \left(1 - \beta + \beta^2\right) - 0.1 \ W{:}H \left(1 + \beta\right) + 1} \tag{6}$$

If the pillar is square in shape, $\beta = 1$, Equation 6 reduces to:

$$\left(\overline{\sigma}_{ef}\right)_{\text{square}} = \overline{\sigma}_v \left[1 - 0.1 \ W{:}H\right] \tag{7}$$

5.1.2.e

If a pillar is long in one dimension; i.e., as β increases, a condition approaching plane strain is achieved. Based on stationary-stress creep considerations (e.g., Van Sambeek [1986]), no creep strain parallel to the long dimension occurs when the deviatoric stress component in that direction is zero; i.e., $\overline{S}_H = 0$ when:

$$\overline{\sigma}_H = \left(\overline{\sigma}_v + \overline{\sigma}_h\right)/2 \tag{8}$$

Using Equation 3 and the relationship $\overline{\sigma}_H = \beta\,\overline{\sigma}_h$, β can be calculated for an effective plane-strain situation (β_{max}):

$$\begin{aligned} \beta\,\overline{\sigma}_h &= \left(\overline{\sigma}_v + \overline{\sigma}_h\right) \\ \beta_{max} &= \frac{\overline{\sigma}_v + \overline{\sigma}_h}{2\overline{\sigma}_h} = \frac{1 + 0.1\ \mathrm{W:H}}{0.2\ \mathrm{W:H}} \end{aligned} \tag{9}$$

Therefore, the average effective stress for long pillars ($W_H \geq \beta_{max}\ W_h$) is:

$$\left(\overline{\sigma}_{ef}\right)_{\beta max} = \frac{\sqrt{3}}{2}\,\overline{\sigma}_v\left[1 - 0.1\ \mathrm{W_h{:}H}\right] \tag{10}$$

Equations 7 and 10 reveal that as W:H becomes large, the effective stress rapidly approaches zero. An alternative approach is shown in the appendix where nonlinear relationship are suggested when W:H > 5.

Pillar Creep Rates

For salt, steady-state creep rates are exponential functions of effective stress, such as:

$$\dot{\varepsilon}^c = A\left(\sigma_{ef}\right)^n \tag{11}$$

where A and n are creep law parameters obtained from laboratory testing: $3 \leq n \leq 6$ and A is site specific and temperature sensitive. The creep-strain rate in a particular direction is defined by generalizing Equation 11 (e.g., Fossum et al. [1988]):

$$\dot{\varepsilon}^c_x = A\left(\overline{\sigma}_{ef}\right)^{n-1}\left(\frac{3}{2}\ \overline{S}_x\right) \tag{12}$$

where:

$\dot{\varepsilon}^c_x$ = creep strain rate in the x-direction

$\overline{S}_x$ = average deviatoric stress component acting in the x-direction.

For a salt pillar, the pillar shortening rate (vertical direction) is therefore:

$$\dot{\varepsilon}_v^c = \left(\frac{\Delta \dot{H}}{H}\right) = A\left(\overline{\sigma}_{ef}\right)^{n-1}\left(\frac{3}{2}\ \overline{S}_v\right) \tag{13}$$

and the pillar lateral expansion rates are:

$$\begin{aligned} \dot{\varepsilon}_h^c &= \left(\frac{\Delta \dot{W}_h}{W_h}\right) = A\left(\overline{\sigma}_{ef}\right)^{n-1}\left(\frac{3}{2}\ \overline{S}_h\right) \\ \dot{\varepsilon}_H^c &= \left(\frac{\Delta \dot{W}_H}{W_H}\right) = A\left(\overline{\sigma}_{ef}\right)^{n-1}\left(\frac{3}{2}\ \overline{S}_H\right) \end{aligned} \tag{14}$$

where $\Delta \dot{H}$, $\Delta \dot{W}_h$, and $\Delta \dot{W}_H$ are rates of change in the respective pillar dimensions. The deviatoric stresses acting in the vertical, $\overline{S}_v$, and horizontal directions, $\overline{S}_h$ and $\overline{S}_H$, are:

$$\begin{aligned} \overline{S}_v &= \overline{\sigma}_v\left(2 - (0.1\ \text{W:H})\,(1 + \beta\,)\right)/3 \\ \overline{S}_h &= \overline{\sigma}_v\left((0.1\ \text{W:H})\,(2 - \beta) - 1\right)/3 \\ \overline{S}_H &= \overline{\sigma}_v\left((0.1\ \text{W:H})\,(2\beta - 1) - 1\right)/3 \end{aligned} \tag{15}$$

Equations 13 through 15 can be used to estimate the effect of changes in pillar size or shape. For example, changing the W:H from 3 to 2 will cause almost a doubling of the pillar shortening rate for the same average vertical stress. Another example is the comparison of square pillars and long pillars for the same minimum pillar width, pillar height, and extraction ratio; the pillar shortening rate for long pillars is less than 50 percent of that for square pillars of the same minimum width.

Pillar Strength

The approach of using average stresses (particularly effective stress) can also be used to inspect the potential for the stress states in pillars to be damaging. Van Sambeek et al. [1993] shows the aptness of a simple dilation limit for salt as:

$$\zeta = \frac{\sqrt{J_2}}{I_1} \begin{cases} \geq 0.27 \text{ dilation-causing stress condition} \\ < 0.27 \text{ nondilating stress condition} \end{cases} \tag{16}$$

where I_1 is the first invariant of the total stress tensor ($I_1 = 3\sigma_m$) and $\sqrt{J_2}$ is the second invariant of the deviatoric stress tensor. Recall $\bar{\sigma}_{ef} = \sqrt{3J_2}$, so $\sqrt{J_2} = \bar{\sigma}_{ef}/\sqrt{3}$. The first invariant of the stress tensor, I_1 is:

$$I_1 = \bar{\sigma}_v + \bar{\sigma}_h + \bar{\sigma}_H = \bar{\sigma}_v \left(1 + 0.1 \text{ W:H} + 0.1 \beta \text{ W:H}\right) \tag{17}$$

where $\beta = W_H{:}W_h$ and $1 \leq \beta \leq \beta_{max}$, as defined previously. Equations 16 and 17 lead to:

$$\zeta = \frac{\sqrt{(0.1 \text{ W:H})^2 \left(1 - \beta + \beta^2\right) - 0.1 \text{ W:H} \left(1 + \beta\right) + 1}}{\sqrt{3} \left[1 + 0.1 \text{ W:H} \left(1 + \beta\right)\right]} \tag{18}$$

For square pillars ($\beta = 1$):

$$\zeta_{(\beta=1)} = \frac{1 - 0.1 \text{ W:H}}{\sqrt{3} \left(1 + 0.2 \text{ W:H}\right)} \tag{19}$$

and for long rectangular pillars ($\beta = \beta_{max}$):

$$\zeta_{(\beta=\beta_{max})} = \frac{1 - 0.1 \text{ W:H}}{\sqrt{3} \left(1 + 0.1 \text{ W:H}\right)} \tag{20}$$

Based on a limiting value of ζ=0.27, dilation is avoided when W:H > 2.75 for square pillars and W:H > 1.05 for long rectangular pillars.

EQUATION VALIDATION

Obviously, any pillar design equation must provide results in agreement with results calculated by other accepted or empirical methods. For this paper, comparison will not be made with other salt pillar design equations in the literature (e.g., those reviewed by Beddoes and Mackintosh [1993]); instead, comparisons will be made to finite-element method (FEM) analyses to demonstrate whether or not the equation oversimplifies the situation.

Two series of finite-element analyses were performed to determine the pillar strain rates and room closure rates for various pillar W:H with constant extraction ratio and pillar height. Figures 1 and 2 show plots of the calculated stresses for the various

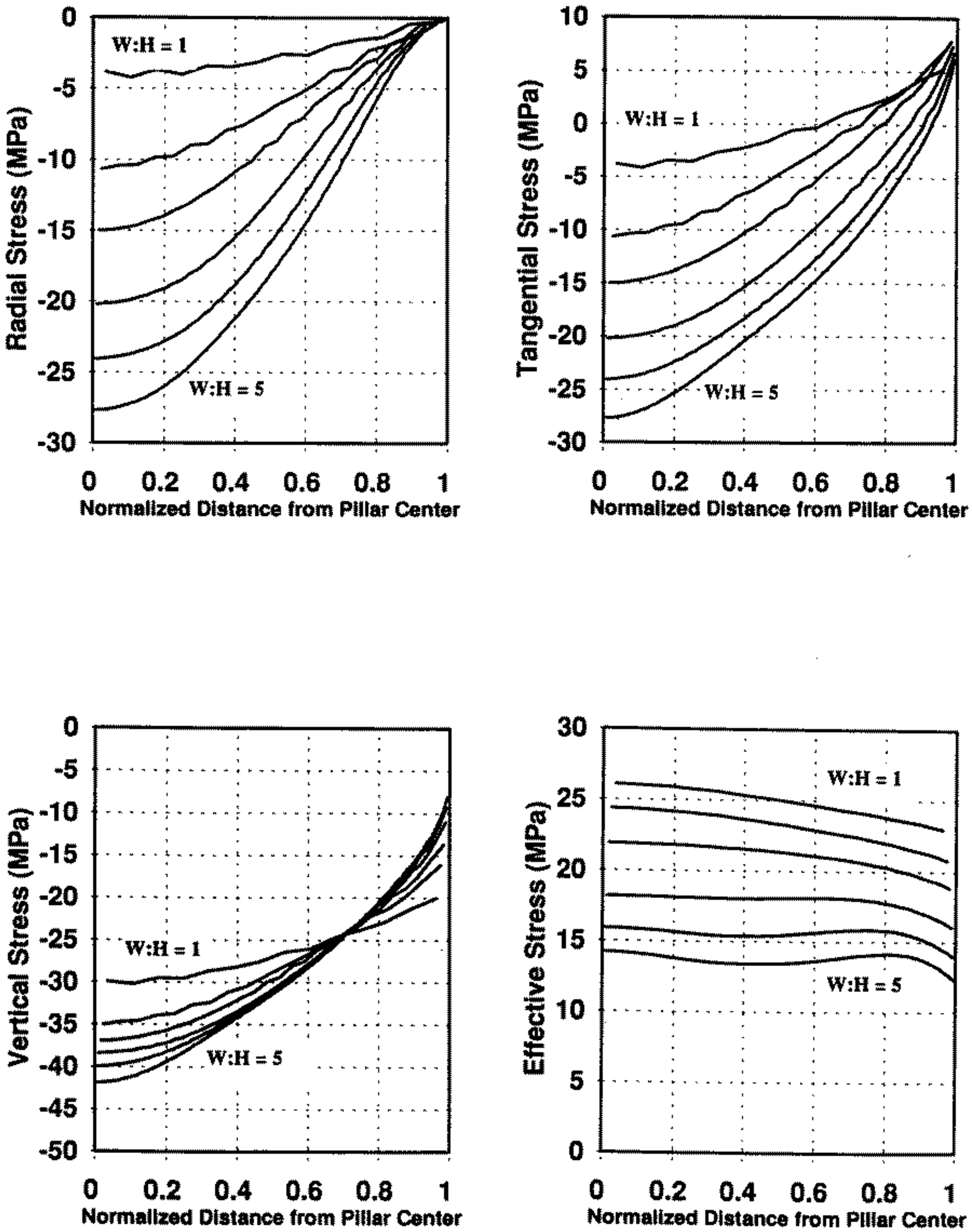

Figure 1. Radial, Tangential, Vertical, and Effective Stress Profiles for Axisymmetric Pillars.

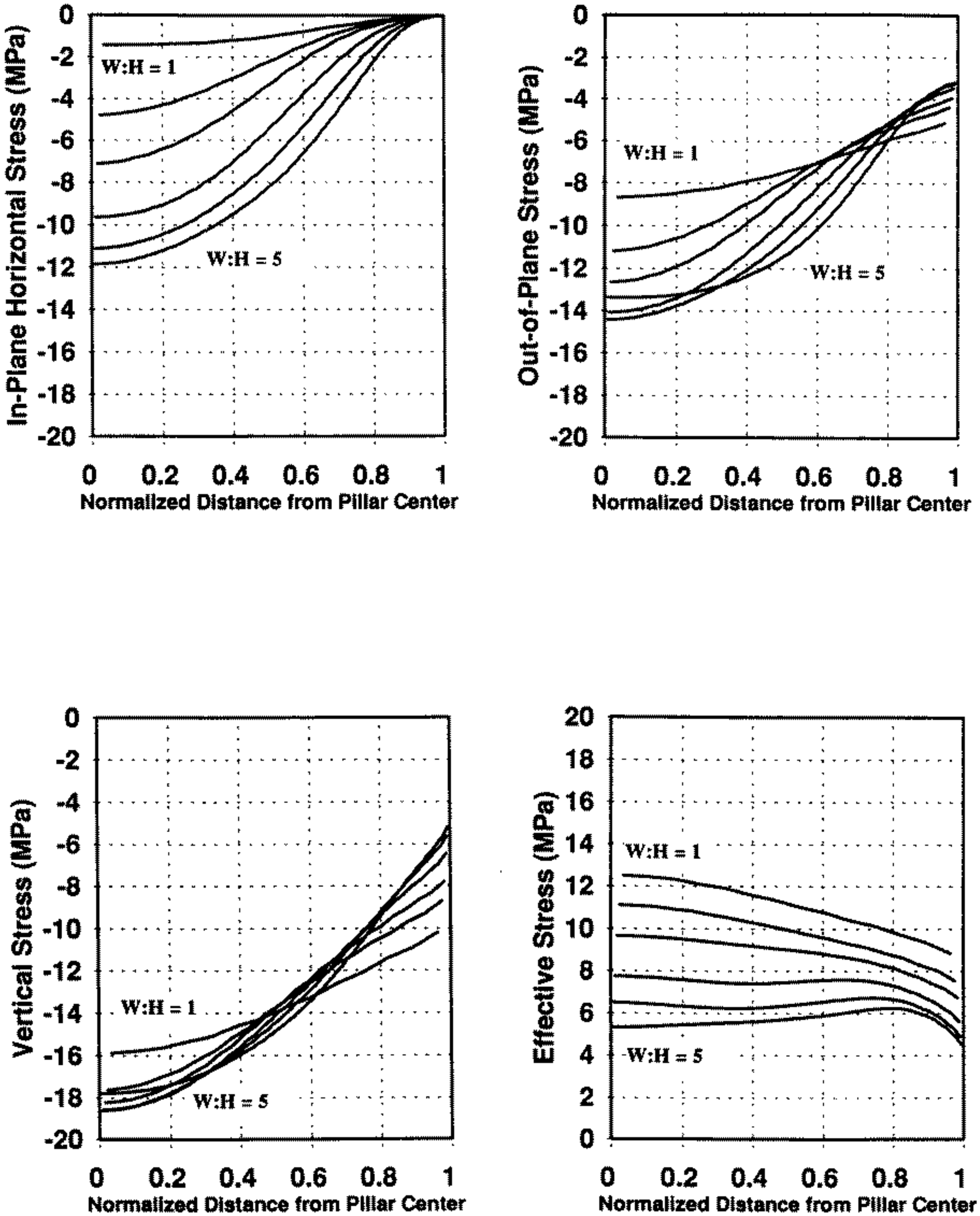

Figure 2. In-Plane and Out-of-Plane Horizontal, Vertical, and Effective Stress Profiles for Plane-Strain Pillars.

5.1.2.e

shaped pillars (axisymmetric and plane strain). Comparisons of normalized average stress values from FEM analyses and the pillar design equation are shown in Figure 3. The values are also shown in Tables 1 and 2. The average vertical, horizontal, and effective stresses within the pillar are integrated average values along the midheight of the pillar. The agreement is excellent, which lends confidence to the use of average pillar stresses for design purposes.

The numerical modeling results were also evaluated in terms of the salt dilatancy criterion ($\sqrt{J_2}:I_1$) for comparison with Equations 19 and 20. The calculated dilatancy factor for axisymmetric and plane-strain pillars for various H:W are shown in Figure 4. In Figure 4, the dilatancy factor is the volume average across the entire pillar width (plane strain) or 85 percent of the pillar area (axisymmetry).

EQUATION VERIFICATION

Before a pillar design equation can be used, it must be compared to actual pillar behavior. Closure information in terms of $\left(\Delta\, \dot{H}/H\right)$ and pillar geometries from nine salt mines, both bedded and domal, were collected for the comparison. Average vertical stresses were calculated based on tributary loading. The expected effective stress was then calculated according to the pillar geometries using Equation 6. The measured closure rates are plotted versus the calculated effective stress in Figure 5. A representative model based on a stress exponent of $n = 5$ is also shown. Scatter exists, and is expected, because no adjustments were made for salt type, age of the pillars, location of pillars within the mines, etc. The only factors considered were the reported extraction ratio, depth, and pillar W:H.

CONCLUSIONS

Pillar design equations were presented which can be applied to comparisons of pillar behavior either from measured or calculated behavior. The equations are obviously approximate; however, they have application when numerical modeling is not practicable. The pillar design equations have limitations; for example, they are not applicable to very slender pillars (W:H < 1), and the linear equations are not suitable for very squat pillars (W:H > 5). While the easiest application is for uniformly sized pillars in a regular pattern over a wide area, the equations can be used in situations involving unequal pillars (such as yield and barrier (bearing) pillars) if proper attention is paid to equilibrating the strain rates by adjusting the average loads on the unequal sized pillars.

Additional data for actual pillars are required to further validate the approach to pillar design. The author would appreciate any information the salt and potash mining industries can provide.

5.1.2.e

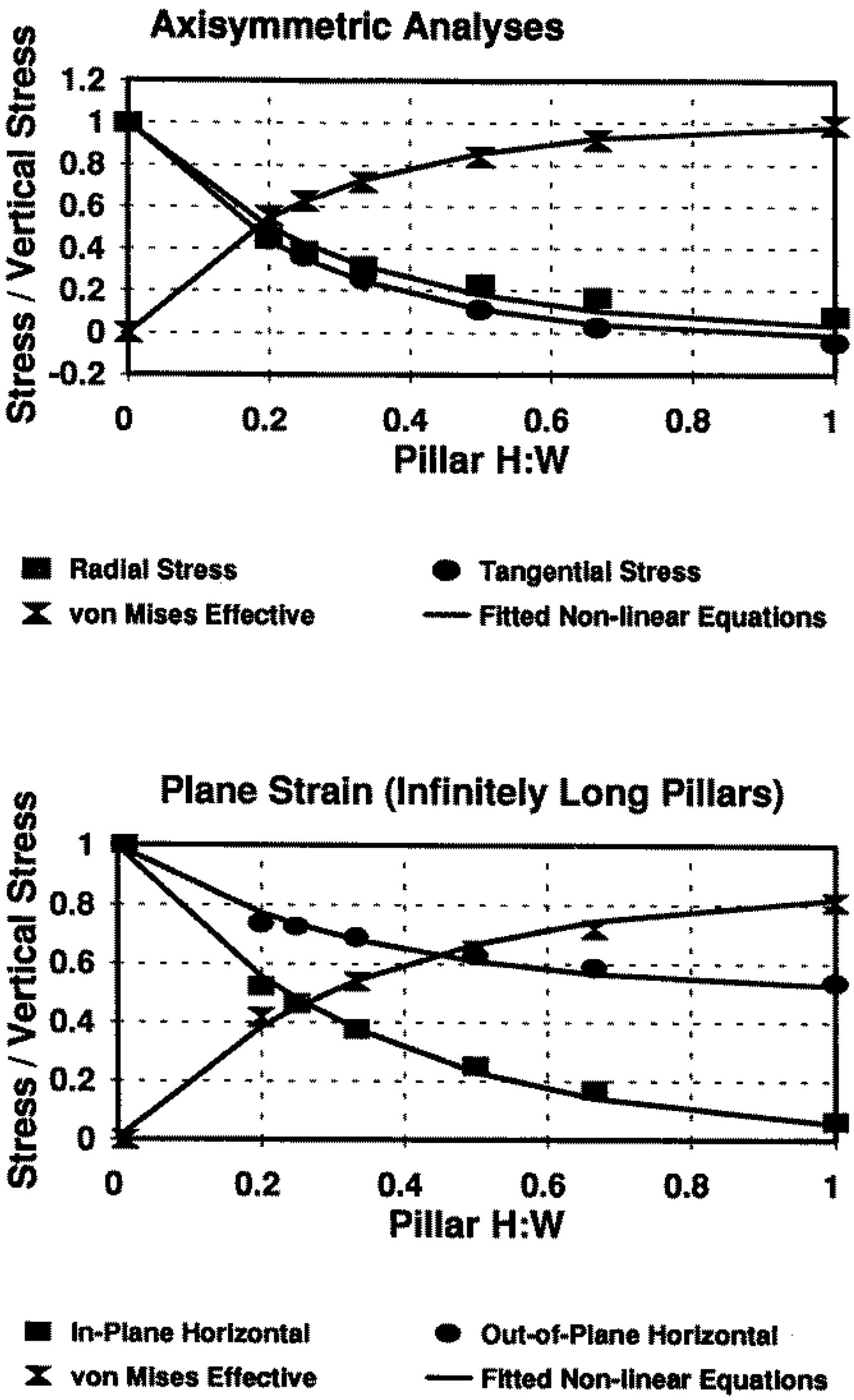

Figure 3. Normalized Average Stress Values for Axisymmetric and Plane-Strain Pillars of Various H:W.

5.1.2.e

Table 1. Average Pillar Stresses in Axisymmetric Pillars

Pillar Shape		Average Stresses From FEM Modeling			Average Stresses From Equations			
					Linear		Exponential	
W:H	H:W	$\bar{\sigma}_{ef}/\bar{\sigma}_v$	$\bar{\sigma}_r/\bar{\sigma}_v$	$\bar{\sigma}_\theta/\bar{\sigma}_v$	$\bar{\sigma}_{eff}/\bar{\sigma}_v$	$\bar{\sigma}_h/\bar{\sigma}_v$	$\bar{\sigma}_{eff}/\bar{\sigma}_v$	$\bar{\sigma}_h/\bar{\sigma}_v$
1	1	0.99	0.08	−0.05	0.90	0.10	0.98	0.02
1.5	0.67	0.92	0.17	0.02	0.85	0.15	0.93	0.07
2	0.5	0.84	0.23	0.11	0.80	0.20	0.86	0.14
3	0.33	0.72	0.33	0.26	0.70	0.30	0.72	0.28
4	0.25	0.63	0.39	0.36	0.60	0.40	0.62	0.38
5	0.2	0.56	0.45	0.44	0.50	0.50	0.54	0.46

Table 2. Average Pillar Stresses in Plane-Strain Pillars

Pillar Shape		Average Stresses From FEM Modeling			Average Stresses From Equations[a]			
					Linear		Exponential	
W:H	H:W	$\bar{\sigma}_{ef}/\bar{\sigma}_v$	$\bar{\sigma}_h/\bar{\sigma}_v$	$\bar{\sigma}_H/\bar{\sigma}_v$	$\bar{\sigma}_{eff}/\bar{\sigma}_v$	$\bar{\sigma}_h/\bar{\sigma}_v$	$\bar{\sigma}_{eff}/\bar{\sigma}_v$	$\bar{\sigma}_h/\bar{\sigma}_v$
1	1	0.81	0.06	0.53	0.78	0.10	0.89	0.11
1.5	0.67	0.72	0.17	0.59	0.74	0.15	0.77	0.23
2	0.5	0.65	0.25	0.63	0.69	0.20	0.66	0.34
3	0.33	0.54	0.38	0.69	0.61	0.30	0.52	0.48
4	0.25	0.47	0.46	0.73	0.52	0.40	0.42	0.58
5	0.2	0.42	0.52	0.74	0.43	0.50	0.35	0.65

(a) NOTE: $\bar{\sigma}_H = (\bar{\sigma}_v + \bar{\sigma}_h)/2$.

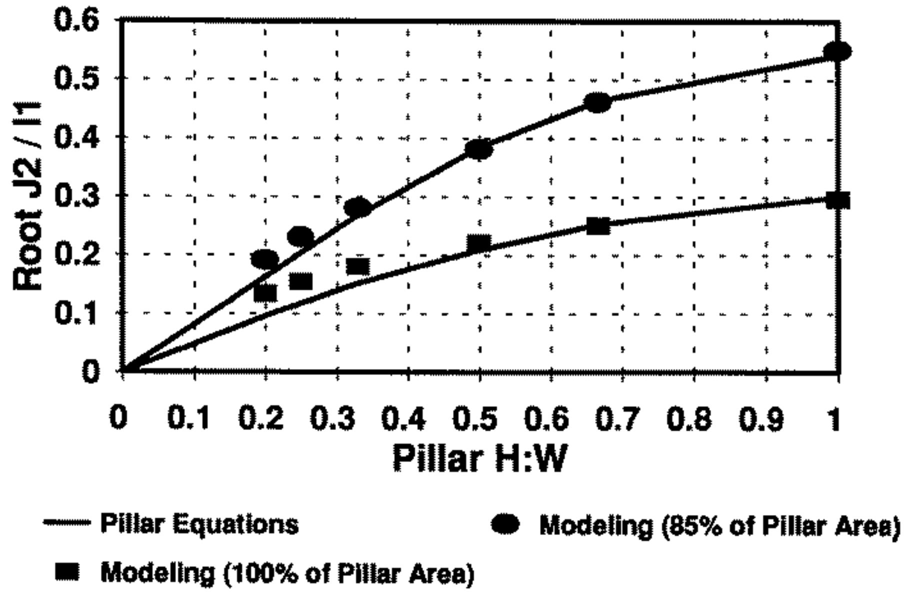

Figure 4. Dilatancy Factors Versus H:W for Axisymmetric and Plane-Strain Pillars.

REFERENCES

Beddoes, R. J. and A.D. Mackintosh, 1993. *A Review and Evaluation of Design Criteria for Use in Evaporite Mines*, prepared under Canada/Nova Scotia Mineral Development Agreement by Golder Associates, Ltd., Calgary, Alberta, Canada.

Fossum, A. F., G. D. Callahan, L. L. Van Sambeek, and P. E. Senseny, 1988. "How Should One-Dimensional Laboratory Equations be Cast Into Three-Dimensional Form?," *Proceedings, 29th U.S. Symposium on Rock Mechanics,* University of Minnesota, Minneapolis, MN, June.

Van Sambeek, L. L., 1984. *Potential Reduction in Surface Subsidence by Backfilling or Flooding the Belle Isle Mine*, RSI–0247, proprietary report prepared by RE/SPEC Inc., Rapid City, SD, for Cargill/Salt Division, Minneapolis, MN.

Van Sambeek, L. L., 1986. *Creep of Rock Salt Under Inhomogeneous Stress Conditions,* Ph.D. Dissertation, T-3207, Colorado School of Mines, Golden, CO.

Van Sambeek, L. L., J. L. Ratigan, and F. D. Hansen, 1993. "Dilatancy of Rock Salt in Laboratory Tests," *International Journal of Rock Mechanics and Mining Sciences & Geomechanics Abstracts*, Vol. 30, No. 7. pp. 735–738.

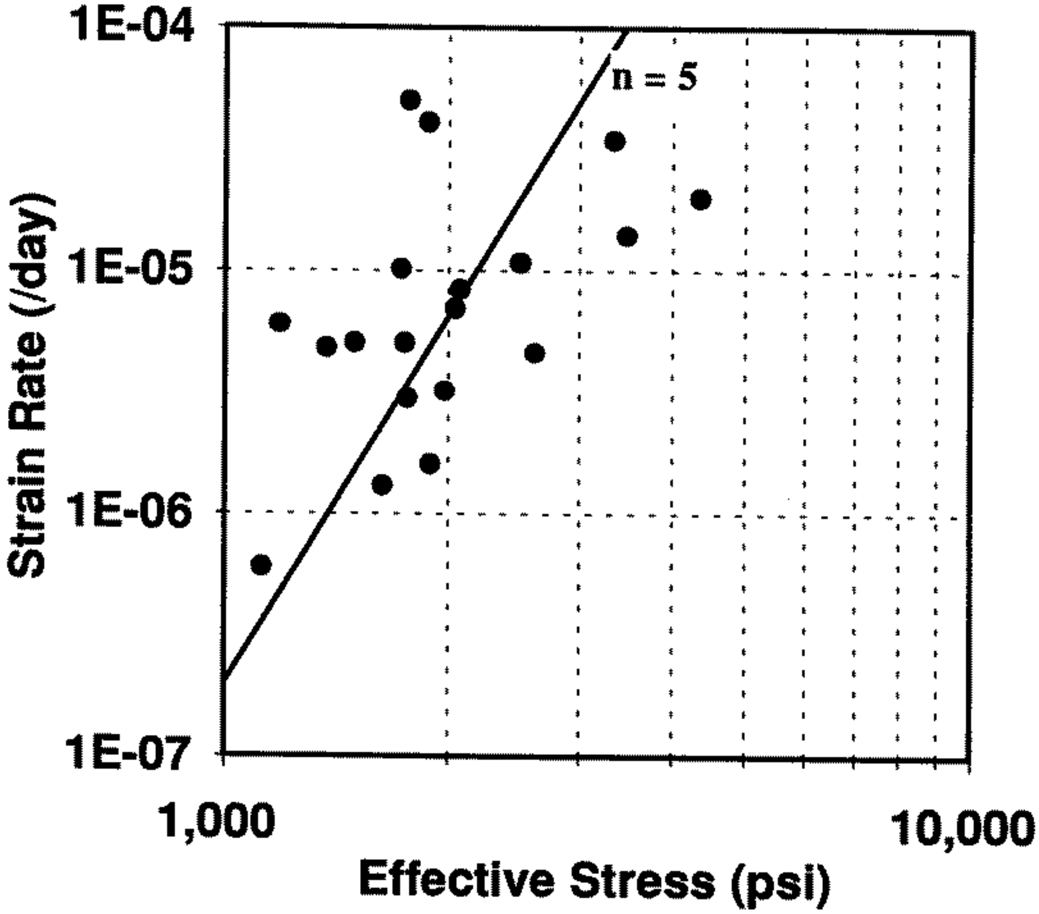

Figure 5. Measured Strain Rates for Pillars in Bedded and Domal Salt Mines Compared to Effective Stress Based on Pillar Equation.

5.1.2.e

APPENDIX A

Linear equations are developed in the main paper to describe the stresses in salt pillars according to their shape. Linear equations are adequate for pillars whose W:H<5, but severely underestimate the effective stress situation for larger W:H. Nonlinear equations were fitted to the calculated stresses to better approximate the stresses in squat pillars. The nonlinear equations use the reciprocal of W:H such that conditions are defined at large W; e.g., H:W=0 as W approaches infinity. The nonlinear equations for the axisymmetric and plane-strain situations are as follows:

<u>Axisymmetric</u>

$$\begin{aligned} \bar{\sigma}_r/\bar{\sigma}_v &= \exp\left(-3.418\,\mathrm{H{:}W}\right) \\ \bar{\sigma}_\theta/\bar{\sigma}_v &= -1.0238 + \exp\left(-3.934\,\mathrm{H{:}W}\right) \\ \bar{\sigma}_{ef}/\bar{\sigma}_v &= 1 - \exp\left(-3.914\,\mathrm{H{:}W}\right) \\ I_1/\bar{\sigma}_v &= 1 + 2\exp\left(-3.83\ \mathrm{H{:}W}\right) \end{aligned} \tag{A-1}$$

<u>Plane Strain</u>

$$\begin{aligned} \bar{\sigma}_h/\bar{\sigma}_v &= \exp\left(-2.931\,\mathrm{H{:}W}\right) \\ \bar{\sigma}_H/\bar{\sigma}_v &= \frac{1}{2}\left(1 + \exp\left(-3.042\,\mathrm{H{:}W}\right)\right) \\ \bar{\sigma}_{ef}/\bar{\sigma}_v &= \frac{\sqrt{3}}{2}\left(1 - \exp\left(-2.940\,\mathrm{H{:}W}\right)\right) \\ I_1/\bar{\sigma}_v &= \frac{3}{2}\left(1 + \exp\left(-2.970\,\mathrm{H{:}W}\right)\right) \end{aligned} \tag{A-2}$$

5.1.2.e

APPENDIX C

THREE-DIMENSIONAL VERIFICATION OF SALT PILLAR DESIGN EQUATION

THREE-DIMENSIONAL VERIFICATION OF SALT PILLAR DESIGN EQUATION

[redacted]

respec@hay.net

RESPEC, Grand Bend, ON, CANADA

[redacted]

[redacted]*@respec.com*

RESPEC, Rapid City, SD, U.S.A.

ABSTRACT

The time-dependent deformational behavior of salt makes the task of salt mine pillar design complex. Current methodologies for pillar design that involve numerical modeling require the commitment of significant computer and human resources to develop an acceptable solution. For this method, preliminary pillar characteristics (size and shape) are based on historical pillar designs, observed behavior, and engineering judgment. Then a worst case–best case approach is used in conjunction with a series of numerical simulations to define the appropriate pillar-design limits. However, as salt mines become deeper and mining economics drive pillar-design decisions, our observations database will become ever smaller. A need exists for simple pillar-design tools that help salt mining operations determine acceptable pillar characteristics and bounds the scope of analysis required to establish a formal pillar design.

Van Sambeek (1996) describes such a tool in the previous conference proceedings. The pillar-design equation developed in that paper is suitable for estimating stresses in square pillars, although assumptions were required to extend its use to rectangular salt pillars. Results from a series of two-dimensional finite element simulations using both axisymmetric and plane-strain analyses could not verify the assumptions used in developing the pillar-design equation for rectangular pillars.

Three-dimensional finite difference simulations of rectangular salt pillars were performed to examine the assumptions used in the extension of the pillar-design equation. The three-dimensional modeling results bolster use of the equation for estimating stress conditions in salt pillars of various shapes and sizes. In particular, this paper (1) reviews the initial pillar-design equation, (2) compares two- and three-dimensional numerical modeling results, and (3) presents equation modifications to improve the agreement with three-dimensional numerical modeling results.

INTRODUCTION

Simple pillar-design equations to calculate the average stresses in salt pillars were developed by Van Sambeek (1996) and presented in the previous conference. A series of two-dimensional axisymmetric and plane-strain numerical modeling analyses showed that the equations adequately reproduced the results of extensive modeling efforts. However, a comprehensive evaluation of the pillar equation was limited by the two-dimensional nature of the previous numerical modeling analyses. Axisymmetric analyses mirror the behavior of square salt pillars, and plane strain analyses simulate the behavior of long salt pillars. The capability to truly examine the behavior of rectangular pillars, which lie between the two extremes, is not available through two-dimensional numerical modeling.

The limitations presented by two-dimensional modeling were addressed for this paper by conducting a series of three-dimensional numerical modeling analyses to examine the behavior of rectangular pillars. The results of the three-dimensional modeling are used to verify the proposed pillar-design equations. The salt pillar-design equations are shown to be capable of reproducing the results of extensive three-dimensional modeling efforts. Use of these equations simplifies comparisons of different pillar sizes and shapes and provides a tool for estimating stress conditions in salt pillars.

TWO-DIMENSIONAL EQUATION REVIEW

Linear and nonlinear equations to predict the average horizontal stresses and the average effective stress for both the axisymmetric and plane-strain analyses are given by Van Sambeek (1996). The average vertical stress in the pillar is used as a normalizing parameter for the other stresses in the various shaped pillars. The average vertical stress ($\bar{\sigma}_v$) when the conditions are met for tributary loading is:

$$\bar{\sigma}_v = \gamma z / (1 - \mathrm{E}) \tag{1}$$

where:

E = areal extraction ratio

z = depth

γ = average stress gradient for the overburden.

Proposed linear equations to calculate stresses in a rectangular-shaped salt pillar at a steady-state stress condition are:

$$\bar{\sigma}_W = \bar{\sigma}_v (0.1\mathrm{W} : \mathrm{H}) \tag{2}$$

$$\bar{\sigma}_L = \bar{\sigma}_v (0.1\mathrm{L} : \mathrm{H}) \tag{3}$$

$$\bar{\sigma}_{ef} = \bar{\sigma}_v \sqrt{(0.1\mathrm{W} : \mathrm{H})^2 (1 - \beta + \beta^2) - 0.1\mathrm{W} : \mathrm{H}(1 + \beta) + 1} \tag{4}$$

where:

W, L = pillar width and length (horizontal dimensions)

H = pillar height (vertical dimension)

$\bar{\sigma}_W, \bar{\sigma}_L$ = average horizontal stresses parallel to the width and length (5)

$\bar{\sigma}_{ef}$ = average effective stress.

$$\beta = \text{minimum} \left| \begin{matrix} L/W \\ \left(\dfrac{1 + 0.1\dfrac{W}{H}}{0.2\dfrac{W}{H}} \right) \end{matrix} \right.$$

Nonlinear, plane-strain versions of the equations (for infinitely long pillars) are as follows:

$$\bar{\sigma}_W / \bar{\sigma}_v = \exp(-2.931\ H:W) \tag{6}$$

$$\bar{\sigma}_L / \bar{\sigma}_v = \frac{1}{2}\left(1 + \exp(-3.042\ H:W)\right) \tag{7}$$

$$\bar{\sigma}_{ef} / \bar{\sigma}_v = \frac{\sqrt{3}}{2}\left(1 - \exp(-2.940\ H:W)\right) \tag{8}$$

Nonlinear, axisymmetric versions of the equations (for square pillars) are as follows:

$$\bar{\sigma}_r / \bar{\sigma}_v = \exp(-3.418\ H:W) \tag{9}$$

$$\bar{\sigma}_\theta / \bar{\sigma}_v = \exp(-3.934\ H:W) \tag{10}$$

$$\bar{\sigma}_{ef} / \bar{\sigma}_v = \frac{\sqrt{3}}{2}\left(1 - \exp(-3.914\ H:W)\right) \tag{11}$$

where:

$\bar{\sigma}_r$ = average radial stress

$\bar{\sigma}_\theta$ = average tangential stress.

THREE-DIMENSIONAL EQUATION DETERMINATION

The pillar-design equations from 5.1.2.e (1996) were checked against average pillar stresses from the three-dimensional finite difference analyses. Forty three-dimensional numerical modeling simulations were performed to determine the pillar stresses for various pillar width to height (W:H) and length to width (L:W = β) ratios. In the analyses, the extraction ratio, pillar height, and saltback thickness were held constant. Average stresses were determined for each pillar and then an equation of the following form was fitted to the two average horizontal stresses and the effective stress:

$$\bar{\sigma} / \bar{\sigma}_v = A_1 + A_2 \exp[A_3(H:W)]\exp[A_4(H:L)] \tag{12}$$

where:

Equation Constant	$\bar{\sigma}_W / \bar{\sigma}_V$	$\bar{\sigma}_L / \bar{\sigma}_V$	$\bar{\sigma}_{ef} / \bar{\sigma}_V$
A_1	0	0	1
A_2	0.94	0.86	–0.90
A_3	–2.84	–0.42	–1.862
A_4	–0.48	–2.46	–1.50

Figures 1 through 3 illustrate the comparison of the normalized average stress values from the numerical modeling analyses and the pillar-design equation. The average vertical, horizontal, and effective stresses were determined at the midheight of the pillar. A comparison of average pillar stresses was made between the earlier version of the pillar-design equation and the equation developed using the three-dimensional numerical modeling results. The linear equations adequately reproduce the three-dimensional stresses for W:H ≤ 4. The nonlinear equations shown above are required for W:H > 4.

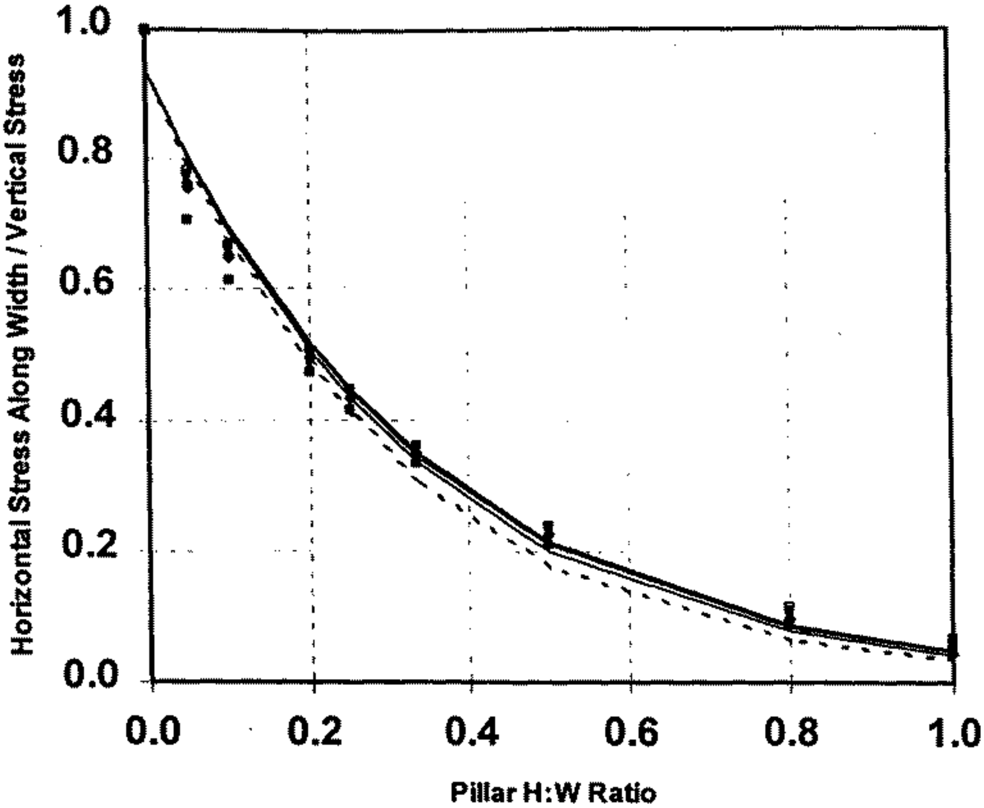

Figure 1. Average Horizontal Stress as a Function of Pillar Height to Width. Beta = 1 for Dashed Curve and Beta = 2 to 5 for Others.

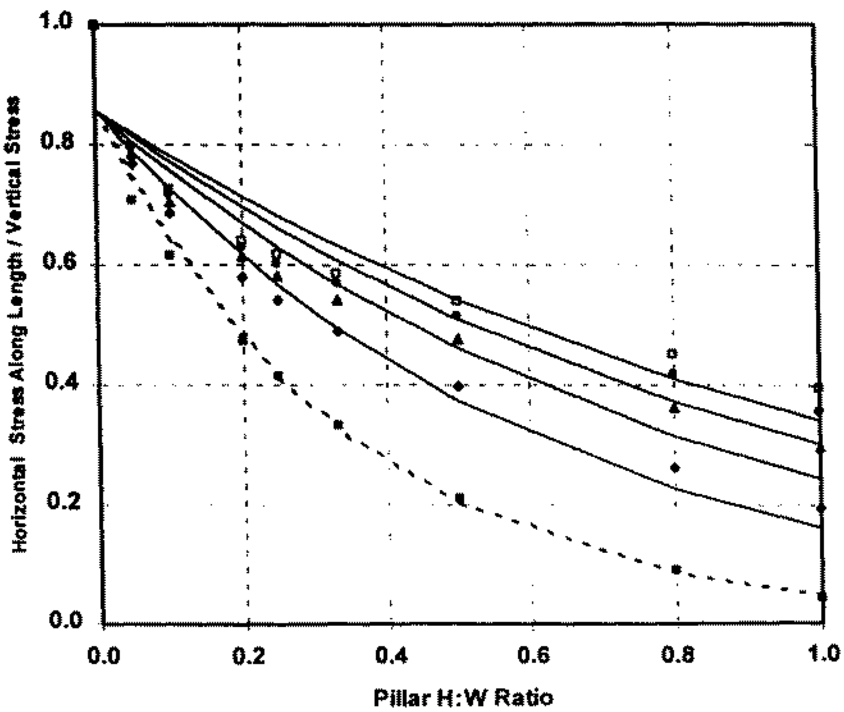

Figure 2. Average Horizontal Stress Along Length of Pillar as a Function of Pillar Height to Width. Dashed Curve for Beta = 1 and Other Curves Progressively Beta = 2 to 5.

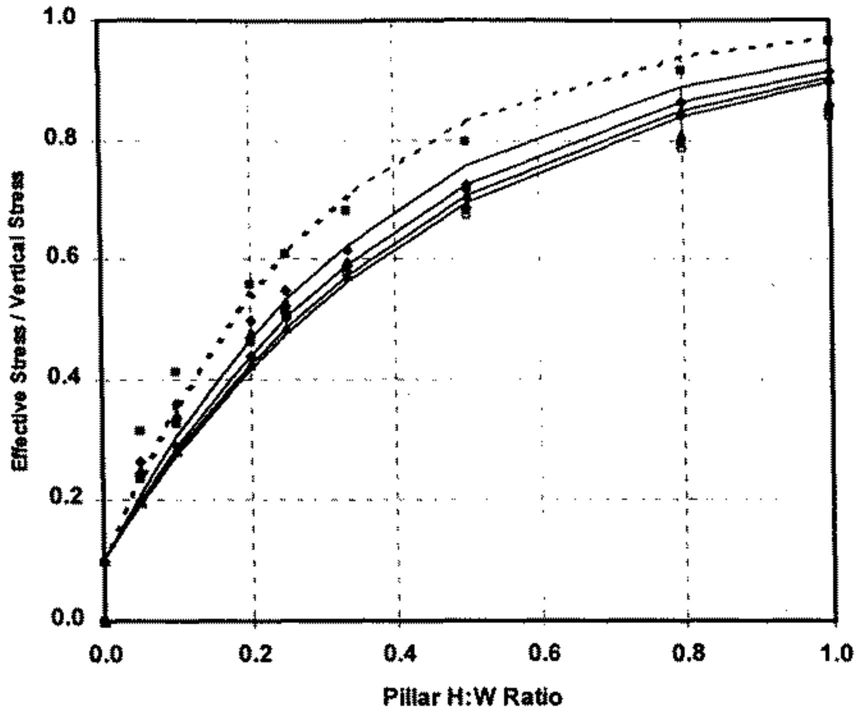

Figure 3. Average Effective Stress in Pillar as a Function of Pillar Height to Width. Dashed Curve for Beta = 1 and Other Curves Progressively Beta = 2 to 5.

CONCLUSION

The previously published salt pillar-design equations were compared to stresses from a series of 40 three-dimensional numerical modeling simulations of rectangular-shaped pillars. The original version of the pillar-design equation had been compared to two-dimensional axisymmetric and plane-strain numerical modeling simulations only. The salt pillar-design equation proposed by Van Sambeek (1996) was found to adequately represent the three-dimensional stresses calculated for rectangular pillars. The same limitations noted in the original paper still apply; use of the salt pillar equation should be restricted to uniformly sized pillars in a regular pattern. Additional work is required to address the condition of yield and bearing pillar configurations or pillars in narrow workings. The equations can, however, be used to estimate the stress conditions in pillars when the pillar deformation rate and constitutive salt properties are known.

REFERENCE

Van Sambeek, L. L., 1996. "Salt Pillar Design Equation," *Proceedings, Fourth Conference of The Mechanical Behavior of Salt,* École Polytechnique de Montréal, Mineral Engineering Department, Québec, Canada, June 17 and 18, M. Aubertin and H. R. Hardy Jr. (eds.), Penn State University, Trans Tech Publications, Clausthal, Germany, 1998, pp. 495–508.

APPENDIX D

REVISED 3D SALT PILLAR EQUATIONS – POWER LAW FORM

Revised 3D Salt Pillar Equations – Power Law Form
November 3, 1999

Because of operational considerations, salt pillars are often rectangular in shape. That is, they are longer in one horizontal dimension (*L*) than the other (*W*). Together with the pillar height (*H*), two ratios define the three-dimensional pillar shape (*W/H* and *L/H* or conversely *H/W* and *L/W*).

Numerical modeling results by 5.1.2.e [redacted] [1999] and 5.1.2.e [redacted] [1996] indicate that stress states within salt pillars can be approximate relative to the average vertical stress in the pillars if the shape of the pillar is considered. A recent reinterpretation of their numerical modeling results has led to a similar conclusion, but a simpler set of equations. For consistency, the pillar is defined as $W < L$.

Average Horizontal Stress Along Width of the Pillar

$$\frac{\overline{\sigma}_W}{\overline{\sigma}_V} = 1 - \left(\frac{H}{W}\right)^{0.43}$$

Average Horizontal Stress Along Length of the Pillar

$$\frac{\overline{\sigma}_L}{\overline{\sigma}_V} = 1 - 0.23\left(\frac{H}{W}\right)^{0.27} - 0.76\left(\frac{H}{L}\right)^{0.43}$$

Average Effective Stress $\left(\sqrt{3J_2}\right)$

$$\frac{\overline{\sigma}_{eff}}{\overline{\sigma}_V} = 0.65\left(\frac{H}{W}\right)^{0.40} + 0.35\left(\frac{H}{L}\right)^{0.35}$$

As is apparent in the equations, when the pillar is very large (W and $L \to \infty$),

$$\overline{\sigma}_W \cong \overline{\sigma}_L \cong \overline{\sigma}_V \text{ and } \overline{\sigma}_{eff} \to 0$$

Conversely, when the pillar is cubic ($W = L = H$),

$$\overline{\sigma}_W \cong \overline{\sigma}_L \cong 0 \text{ and } \overline{\sigma}_{eff} \to \overline{\sigma}_V$$

Plots of the equations superimposed on the numerical modeling results are shown in the attached figures.

5.1.2.e [redacted]

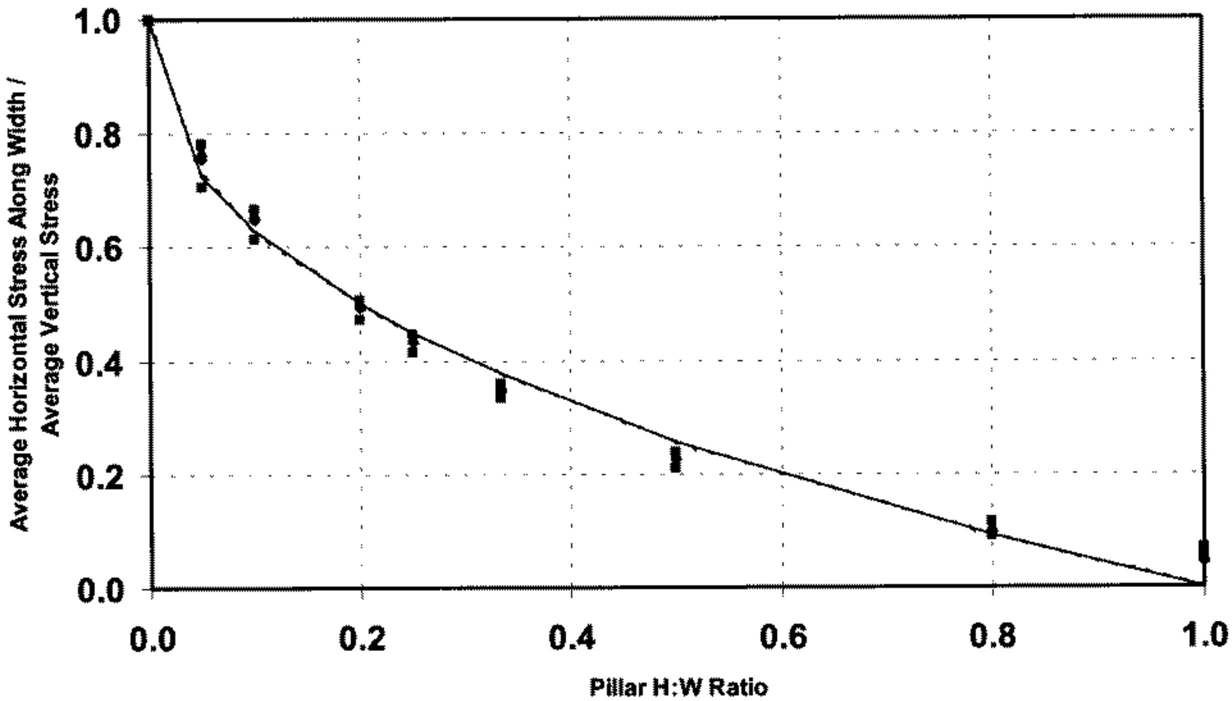

Average Horizontal Stress along Width Normalized by Average Vertical Stress

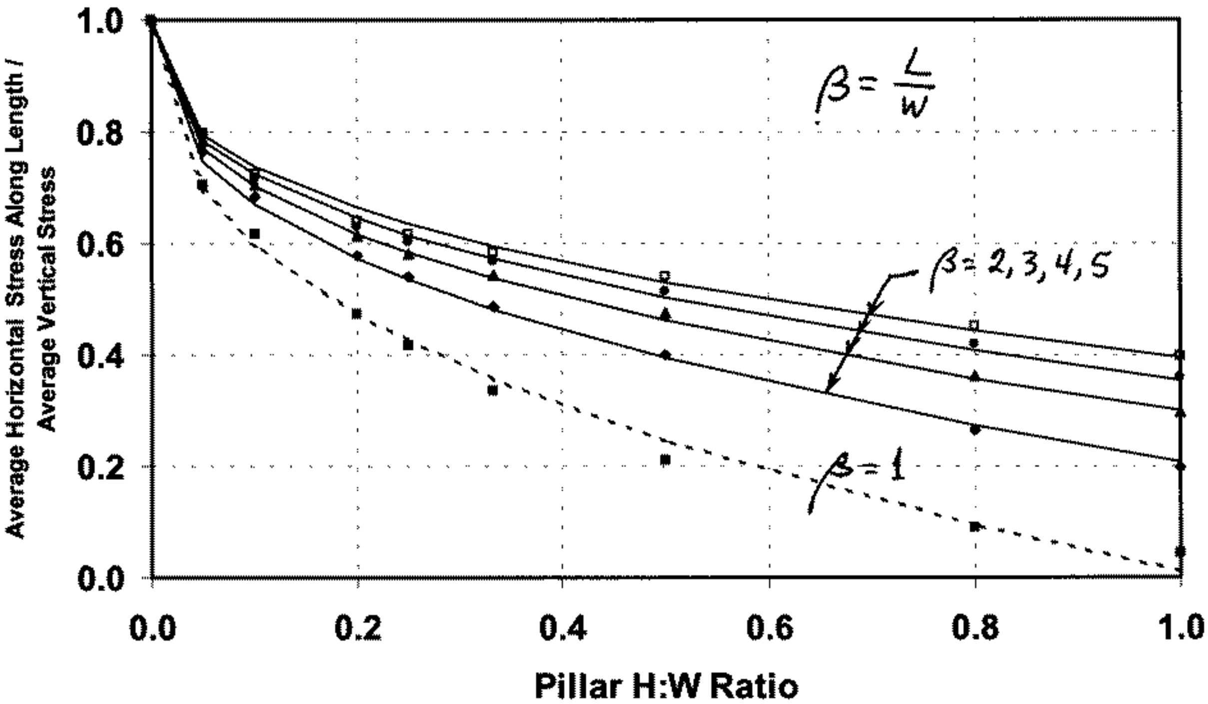

Average Horizontal Stress along Length Normalized by Average Vertical Stress

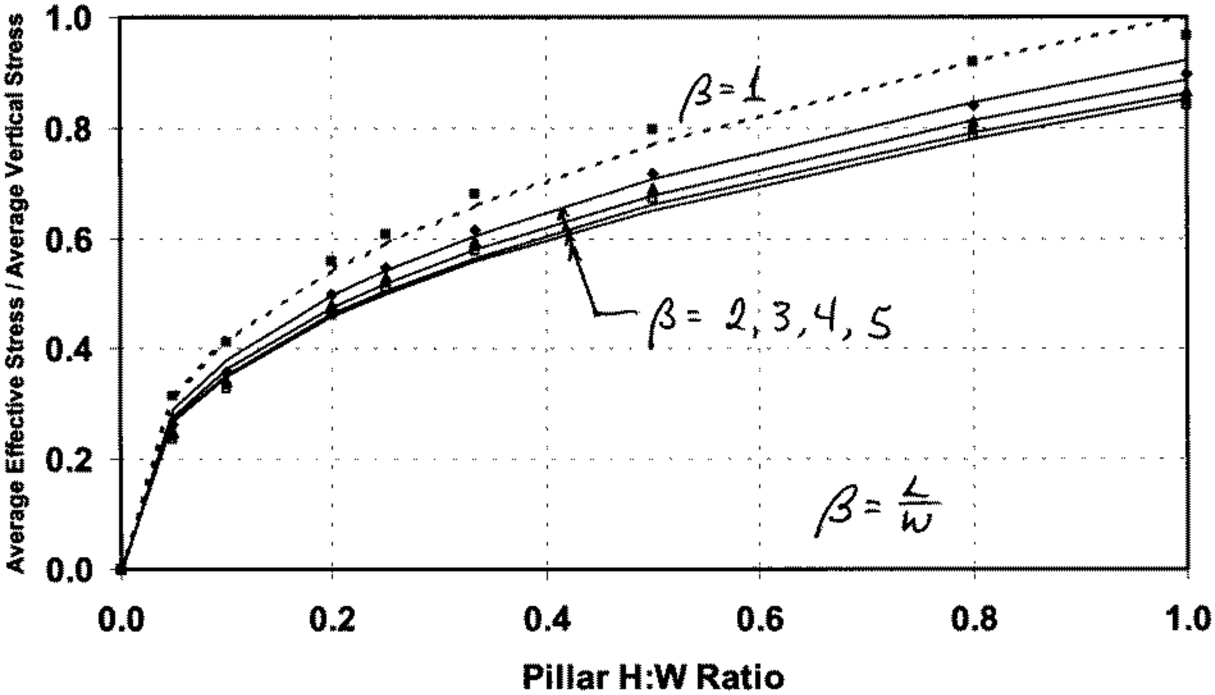

Average Effective Stress Normalized by Average Vertical Stress